Developmental Biology 435 (2018) 26–40

Contents lists available at ScienceDirect

Developmental Biology

journal homepage: www.elsevier.com/locate/developmentalbiology

An organizing role for the TGF-β signaling pathway in axes formation of the annelid *Capitella teleta*

Alexis R. Lanza, Elaine C. Seaver*

Whitney Laboratory for Marine Bioscience, University of Florida, 9505 Ocean Shore Blvd., St. Augustine, Fl 32080, USA

ARTICLE INFO

Keywords:
BMP
TGF-β
Organizer activity
Annelid
Axes formation
Spiralian

ABSTRACT

Embryonic organizers are signaling centers that coordinate developmental events within an embryo. Localized to either an individual cell or group of cells, embryonic organizing activity induces the specification of other cells in the embryo and can influence formation of body axes. In the spiralian *Capitella teleta*, previous cell deletion studies have shown that organizing activity is localized to a single cell, 2d, and this cell induces the formation of the dorsal-ventral axis and bilateral symmetry. In this study, we attempt to identify the signaling pathway responsible for the organizing activity of 2d. Embryos at stages when organizing activity is occurring were exposed to various small molecule inhibitors that selectively inhibited either the Activin/Nodal or the BMP branch of the TGF-β signaling pathway. Embryos were then raised to larval stages, and scored for axial anomalies analogous to 2d ablated phenotypes. Our results show that interference with the Activin/Nodal pathway through a short three hour exposure to the inhibitor SB431542 results in larvae that lack bilateral symmetry and a detectable dorsal-ventral axis. However, interference with the BMP signaling pathway through exposure to the inhibitors DMH1 and dorsomorphin dihydrochloride does not appear to play a role in specification by 2d of the dorsal-ventral axis or bilateral symmetry. Our findings highlight species differences in how the molecular architecture of the conserved TGF-β superfamily signaling pathway components was utilized to mediate the organizing activity signal during early spiralian development.

1. Introduction

Formation of animal body axes (anterior-posterior, dorsal-ventral, left-right) is crucial in the development of an embryo. For many species, this is orchestrated by a central signaling center known as the organizer, which choreographs developmental events essential for body patterning. Both the number of cells and the timing of action that constitute the organizer differ across species. For example, in chordates such as *Xenopus laevis* (Gerhart et al., 1991) and *Danio rerio* (Kimmel et al., 1990; Shih and Fraser, 1996), the cephalochordate *Branchiostoma floridae* (Onai et al., 2010) as well as in the cnidarian *Nematostella vectensis* (Kraus et al., 2016), organizing activity is localized to a group of cells at the blastopore lip during gastrulation. However, in mollusks such as *Ilyanassa obsoleta* (Clement, 1976, 1962), and *Lymnaea stagnalis* (Martindale, 1986), a single cell in the early cleavage stage embryo has organizing activity. Furthermore, the number of axes induced by an organizer differs across species; whereas in some bilaterians all three axes are specified by the organizer, in others it is only dorsal-ventral and left-right axes (Goldstein and Freeman, 1997).

In spiralians, a group of animals that include mollusks, annelids, nemerteans, etc., the organizer is generally localized to a single cell in the early cleavage stage embryo. Spiralian embryonic development follows a highly conserved, stereotypic cleavage program named spiral cleavage. This conservation in cleavage pattern across taxa allows for the identification of individual cells and for intertaxonomic comparisons, which is facilitated by a standard nomenclature. In some spiralian embryos, the first two divisions produce cells of unequal sizes that result in the formation of four blastomeres called A, B, C, and D, the largest of which is the D macromere. Together, descendants of these four blastomeres define the four quadrants of the embryo. During the third cleavage division, each cell gives rise to one daughter cell at the vegetal pole, the macromeres 1A, 1B, 1C, and 1D, as well as typically smaller daughter cells towards the animal pole, called micromeres 1a, 1b, 1c, and 1d. The birth of these micromeres, known as the 1st quartet micromeres, occurs in a clockwise direction with respect to the position of the macromere when viewed from the animal pole. The formation of each subsequent quartet of micromeres occurs in cycles of counter-clockwise and clockwise directions. During the fourth cleavage division from the eight to the sixteen-cell stage, both the macromeres

* Corresponding author.
E-mail address: seaver@whitney.ufl.edu (E.C. Seaver).

https://doi.org/10.1016/j.ydbio.2018.01.004
Received 30 August 2017; Received in revised form 9 January 2018; Accepted 9 January 2018
Available online 11 January 2018

and the 1st quartet micromeres divide. Macromeres 1A, 1B, 1C and 1D each divide to form macromeres 2A, 2B, 2C, and 2D respectively, and the 2nd quartet micromeres 2a, 2b, 2c, and 2d, respectively. Meanwhile, the micromeres of the 1st quartet, 1a, 1b, 1c, and 1d each divide to generate two daughter micromeres – $1a^1$ and $1a^2$, $1b^1$ and $1b^2$, $1c^1$ and $1c^2$, $1d^1$ and $1d^2$. Cells with a '1' superscript are positioned towards the animal pole of the embryo with respect to their sister cell (designated by a superscript '2'). Subsequent cleavages of the macromeres occur following a similar spiral cleavage pattern through to the onset of gastrulation.

Aside from a shared cleavage program, spiralians also possess a conserved fate map in which structures are generally derived from homologous cells (Ackermann et al., 2005; Hejnol, 2010; Meyer et al., 2010). For example, larval eyes in many species are derived from the 1st quartet cells 1a and 1c, trunk mesoderm from cell 4d, and a majority of the trunk ectoderm is derived from cell 2d. Furthermore, it has also been demonstrated that the D quadrant possesses the ability to establish dorsal-ventral polarity in embryos (Dorresteijn et al., 1987; Hejnol, 2010; Henry and Martindale, 1987; Render, 1989, 1983).

It is the spiralian D quadrant that generally gives rise to a single cell organizer that functions in patterning the embryo during early cleavage stages. Despite conservation in quadrant identity, the precise timing of the organizing signal and its cellular identity varies among species. In mollusks such as the mudsnail *Ilyanassa obsoleta* and the limpet *Patella vulgata,* the organizing signal is required through the 32 cell stage and is localized to cell 3D (Clement, 1962; Damen and Dictus, 1996; Lambert and Nagy, 2003). In the slipper shell snail *Crepidula fornicata,* the organizing activity is required one cleavage division later at the 64 cell stage as cell 4d (Henry and Perry, 2008; Henry et al., 2006).

Another spiralian in which organizer activity is localized to the D quadrant is in the annelid, *Capitella teleta* (Amiel et al., 2013). In *C.* teleta, organizing activity patterns the dorsal-ventral axis and establishes bilateral symmetry. Amiel et al. demonstrated that cell 2d, which is present in the 16 cell stage embryo a day prior to gastrulation, is required for organizing activity. Descendants of cell 2d give rise to the ectoderm of the larval trunk and pygidium (Meyer and Seaver, 2010). However, laser deletion of cell 2d not only results in the loss of 2d and its descendants, but also leads to disorganization of the head (Amiel et al., 2013). The structures of the head arise from first quartet micromeres (Meyer et al., 2010; Meyer and Seaver, 2010), suggesting that cell 2d is capable of influencing the fate of its neighbors and is ultimately essential for bilateral symmetry and dorsal-ventral axis formation. Such an effect on the developmental fate of surrounding cells is not seen following the deletion of both daughter cells of 2d, $2d^1$ + $2d^2$ at the 32 cell stage (Amiel et al., 2013). This further indicates that the requirement for organizing activity ceases after the 16-cell stage.

Initial investigations into the nature of the molecular signals mediated by the organizer cell suggest that D quadrant specification and axes formation has been linked to activation of the ERK/MAPK signaling pathway in mollusks. For example, in mollusks such as *Ilyanassa fornicata* (Lambert and Nagy, 2001), *Crepidula fornicata* (Henry and Perry, 2008), *Tectura scutum* (Lambert and Nagy, 2003), and *Haliotis asinina* (Koop et al., 2007), activation of MAPK is observed in D quadrant blastomeres, and inhibition of ERK phosphorylation in these embryos leads to loss of axial organization in larvae. In contrast, in the annelids *Platynereis dumerilii* (Pfeifer et al., 2014) and *C. teleta* (Amiel et al., 2013), it appears that a distinct molecular mechanism is used. When either *P. dumerilii* or *C. teleta* embryos are exposed to U0126, a MEK-1 and MEK-2 inhibitor, the resulting larvae have normal body axes organization (Amiel et al., 2013; Pfeifer et al., 2014). Therefore, there appears to be variation in the molecular mechanisms utilized by spiralians to mediate the organizer signal.

TGF-β superfamily signaling regulates a variety of developmental processes, and has a conserved role in patterning the dorsal-ventral body axis (Wu and Hill, 2009). There are two distinct branches within the TGF-β superfamily; the branch activated by ligands such as TGF-β, Nodal, and Activin will here on be referred to as the Activin/Nodal pathway and the branch activated by ligands such as BMP5-8, BMP2/4, and ADMP will here on be referred to as the BMP pathway. Furthermore, both possess branch-specific signal transduction components. Dimerized ligands in both the Activin/Nodal and BMP branches mediate signaling by binding to a type II transmembrane serine/threonine kinase receptor. Upon ligand binding, a heterotetramer forms with a type I serine/threonine kinase receptor, which is subsequently activated via a transphosphorylation event. This results in the intracellular activation of downstream Smads via phosphorylation, and complex formation with the mediator Smad4. Following translocation into the nucleus, the complex regulates gene expression, in some cases by binding to DNA directly. Regulation of the TGF-β superfamily is also facilitated by secreted agonists and antagonists, such as chordin and gremlin, and by membrane-associated co-receptors (Weiss and Attisano, 2013). In *C. teleta,* all components necessary for signaling via both branches of the TGF-β superfamily are present within the genome, as was recently reported by Kenny et al. (2014).

In this study, we investigate the identity of the molecular signal sent by 2d that induces the formation of the dorsal-ventral axis and bilateral symmetry in *C. teleta*. The Activin/Nodal and BMP signaling pathways are investigated using small molecule chemical inhibitors that target the type I receptors in each of the two branches of this signaling pathway. Embryos at stages during which organizing activity occurs were exposed to either an Activin/Nodal (SB-431542) or BMP (dorsomorphin dihydrochloride; DMH1) pathway inhibitor, raised to larval stages, and scored for axial anomalies using morphological and molecular markers. Further analyses of larval phenotypes were also conducted using lineage tracing.

2. Materials and methods

2.1. Animal care

A laboratory colony of *C. teleta* adults were kept and maintained as previously described (Seaver et al., 2005). Broods of early stage embryos were obtained by mating gravid females with sexually mature males as previously described (Yamaguchi et al., 2016).

2.2. Drug treatments

Each brood of early stage embryos was divided into experimental and control conditions. Embryos were exposed to a DMSO solvent control or drug inhibitor for approximately 3 h during two early-cleavage-stage time windows: the 4–32 cell stage and the 32–256 cell stage. For inhibition of the Activin/Nodal signaling pathway, SB431542 (Santa Cruz; Cat No: SC-204265A), a chemical inhibitor that prevents the phosphorylation of ALK4, ALK5, ALK7 Activin/Nodal type 1 receptors, was used. For BMP inhibition, two different chemical inhibitors were used: DMH1 (Sigma; Cat No: D8946), an inhibitor of ALK2 a BMP type 1 receptor, or dorsomorphin dihydrochloride (Tocris; Cat No: 3093), an inhibitor of both ALK2 and ALK3 BMP type 1 receptors. SB431542, DMH1, and dorsomorphin dihydrochloride were each diluted in 100% Dimethyl sulfoxide (DMSO) to a 10 mM stock. Working concentrations were diluted in filtered seawater (FSW). Initial experiments included exposure to the following range of drug concentrations: 1–100 μM for SB43154; 10–40 μM for DMH1; 5–10 μM for dorsomorphin dihydrochloride. The lowest concentration at which there was a consistently reproducible larval phenotype was selected for detailed analysis. To monitor for any potential toxic effects of the solvent, control embryos were exposed to DMSO in FSW at a concentration equivalent to the experimental condition (0.01–1% DMSO). Experimental drug concentrations used were SB431542 at 40 μM, DMH1 at 40 μM, and dorsomorphin dihydrochloride at 5 μM. Following exposure, embryos were washed with FSW for 4 × 1 min,

followed by 4 × 15 min to remove drug or DMSO. Embryos were then raised to larval stage 6 (~ 6 days) or larval stage 8 (~ 8 days) at 19 °C in FSW with 60 μg/ml penicillin (Sigma-Aldrich Co., St Louis, MO, USA) and 50 μg/ml streptomycin (Sigma-Aldrich Co., St Louis, MO, USA). Specimens were fixed for either immunolabeling or whole-mount *in situ* hybridization as described below.

2.3. Immunolabeling

To prevent larval muscle contractions upon fixation, larvae were relaxed for 10 min in a 1:1 dilution of 0.37 M $MgCl_2$:FSW followed by fixation with 3.7% paraformaldehyde (PFA) in FSW for 30 min. For embryos, a three minute membrane softening treatment consisting of a 1:1 solution of 1 M sucrose and 0.25 M sodium citrate was used prior to fixation with 3.7% PFA in FSW for 30 min. Fixation was terminated via 2× quick exchanges with phosphate-buffered saline (PBS), followed by 2× washes in PBS with 0.1% Triton X-100 (PBT). Animals were either used immediately for immunolabeling and phalloidin staining, or stored in PBS at 4 °C for up to 1 month. Fixed animals were treated with a blocking solution of PBT+10% heat-inactivated goat serum (Sigma-Aldrich Co., St Louis, MO, USA) for 1 h at room temperature. Primary antibody in blocking solution was then added and incubated at 4 °C overnight (O/N). The primary antibodies used were 1:400 dilution of mouse anti-acetylated tubulin (6-11b-1, Sigma-Aldrich Co., St Louis, MO, USA), 1:500 dilution of mouse anti-histone (Millipore, Cat No. MABE71), and rabbit anti-phospho-Smad1/Samd5/Smad9 (Cell Signaling, Cat No. 13820S; 9516).

Animals were washed with PBT several times to remove primary antibody and then incubated with a secondary antibody in blocking solution for three hours at room temperature (RT). Goat anti-mouse or secondary antibody conjugated with a fluorescent tag was diluted 1:400 in PBT, (Molecular Probes, Gran Island, NY). Following incubation in secondary antibody, animals were again washed with PBT several times, and cell membranes and larval muscles were visualized by staining with 1:200 Alexa Fluor 488-phalloidin (Sigma-Aldrich Co., St Louis, MO, USA).

2.4. Cloning of Ct-ALK4/5/7, Ct-activin receptor 2, Ct-SMAD2/3 and Ct-ADMP genes

PCR was used to isolate fragments of the following genes using the following primers: *Ct-ALK4/5/7* (NCBI accession numbers EY573133/EY573134) with 5′-CATGGCACACTTTGAGTCGT-3′ as the forward primer and 5′-CAGCACAATGCAGTCTGAAA-3′ as the reverse primer; *Ct-Activin Receptor 2* (NCBI accession number MG762737) with 5′-GAGGCCTATAAGCATGAGTGCG-3′ as the forward primer and 5′-GCGACTCTTTCCTGCGTATCG-3′ as the reverse primer; *Ct-SMAD2/3* (NCBI accession number EY550106) with 5′-GGCGTTCAACCTGAAGAGAG-3′ as the forward primer and 5′-TATCTTTGAGCGCAGTCCCT-3′ as the reverse primer; *Ct-ADMP* (NCBI accession number: EY58275) with 5′-TGCATGGATAAACGACTCCA-3′ as a forward primer and 5′-CCGTCTGGATCGGAGATAAA-3′ as the reverse primer.

Amplified fragments were 923 bp (*Ct-ALK4/5/7*), 1082 bp (*Ct-Activin Receptor 2*), approx. 1450 bp (*Ct-SMAD2/3*), and 966 bp (*Ct-ADMP*) and these were subcloned into pGEM-T Easy vector (Promega, Madison, WI, USA), and sequenced at the University of Hawaii or Macrogen Corp (Maryland).

2.5. Whole mount in situ hybridization

Whole mount *in situ* hybridization (WISH) was performed following previously published protocols for *C. teleta* (Seaver et al., 2005, 2001). Animals prepared for WISH where fixed in 3.7% PFA:FSW at 4 °C overnight. Following fixation, animals were washed 3× in PBT, 2× in diH_2O, and then dehydrated in a series of increasing concentrations of methanol in milliQ water (25%, 50%, 75%, 100%). Animals were stored in 100% methanol at −20 °C for a minimum of 12 h before using them in the *in situ* hybridization protocol. Animals were hybridized for 72 h at 65 °C with each probe. Digoxigenin-labeled riboprobes for all genes were generated with either the SP6 or T7 MEGAscript kit (Ambion, Inc., Austin, TX, USA). Probe lengths and concentrations used were as follows: *Ct-ALK4/5/7,* 923 bp, 2 ng/μl; *Ct-Activin Receptor 2*, 1082 bp, 2 ng/μl; *Ct-SMAD2/3*, 1450 bp, 2 ng/μl; *CapI-elav1* (NCBI accession number FJ830866), 820 bp, 0.5 ng/μl; *CapI-foxA* (NCBI accession number EF651787), 929 bp, 0.2 ng/μl; *Ct-ADMP,* 966 bp, 2 ng/μl; *Ct-foxAB* (NCBI accession number EY608429), 1175 bp, 1 ng/μl. Detection of the DIG-labeled RNA probe was either carried out via a colorimetric development protocol using anti-digoxigenin-AP, an alkaline phosphate buffer and NBT/BCIP (USBiological, Salem, MA, USA) (Seaver et al., 2001) or a fluorescent development protocol using anti-digoxigenin-POD (1:500), a tyramide buffer (2 M NaCl, 0.1 M Boric Acid, pH 8.5) followed by a 10 min incubation with a tyramide development solution (tyramide buffer, 1:1000 IPBA 20 mg/ml stock diluted in DMF, 1:10000 3% H_2O_2) with 1:1000 rhodamine-conjugated tyramide (Hopman et al., 1998). In both cases, development was terminated by repeated washes.

2.6. Lineage tracing

To soften the egg membrane prior to microinjection, embryos at the 4 cell stage were treated with a freshly made 1:1 solution of 1 M sucrose and 0.25 M sodium citrate for 15 s, followed by three quick washes with an excess volume of FSW, following Meyer et al. (2010). Embryos were then placed into either 0.4% DMSO as a drug treatment control or 40 μM SB431542 suspended in 0.4% DMSO as per the drug treatment protocol described above. Individual blastomeres were pressure injected with a solution of 1 part DiC_{18} (Invitrogen, Carlsbad, CA, USA) saturated in ethanol in 19 parts soybean oil using pulled quartz glass needles (Sutter Instruments; Item No: QF100-70-10). After microinjections, treated embryos were washed out of drug/DMSO with FSW. Microinjected embryos were raised to larval stage 6 at 19 °C in FSW with 60 μg/ml penicillin (Sigma-Aldrich Co., St Louis, MO, USA) and 50 μg/ml streptomycin (Sigma-Aldrich Co., St Louis, MO, USA), whereupon larvae were imaged live using an Imager M2 microscope paired with an Axiocam 506 Mono (Zeiss, Gottingen, Germany).

2.7. Lucifer Yellow microinjections

The outer egg membrane was softened in embryos prior to microinjection as described for lineage tracing. Blastomere 2d was pressure injected with a mixture of 1:1 Lucifer Yellow (ThermoFisher Scientific, Cat No. L453): Texas red dextran (ThermoFisher Scientific, Cat No. D1828) as a 5% solution diluted in diH_2O. Injectant was delivered through quartz glass needles (Sutter Instruments; Item No: QF100-70-10). Each injected embryo was visually monitored for spread of fluorescence for a minimum of 15 min and often for the remainder of the cell cycle of 2d. Embryos were visually monitored for any damage due to microinjection and such cases were removed from the analysis. Examination of dye coupling was performed on a stereomicroscope. Four independent replicates of the experiment were performed. After microinjection, embryos were imaged live by confocal microscopy.

2.8. Microscopy and imaging

For imaging, animals were placed in 80% glycerol in 1× PBS plus 0.125 μg/ml Hoechst, a DNA visualization stain. Specimens were viewed from multiple orientations when analyzed for features indicating the presence of an anterior-posterior axis, dorsal-ventral axis and

bilateral symmetry. Following whole mount *in situ* hybridization, specimens were imaged by compound light microscopy using an Axioskop 2 motplus compound microscope (Zeiss, Gottingen, Germany) and a SPOT FLEX digital camera along with the SPOT imaging software (Diagnostic Instruments, Inc., SterlingHeights, MI). Images were processed using Helicon Focus (Helicon Soft Ltd., Kharkov, Ukraine) and Adobe Photoshop CS6 (version 13.0). Following microinjection, fluorescent staining, or immunohistochemistry, animals were imaged using either a Zeiss LSM 710 confocal microscope or Imager M2 microscope paired with an Axiocam 506 Mono (Zeiss, Gottingen, Germany). 3D reconstructions were generated using Fiji (Fiji is Just ImageJ) (Schindelin et al., 2012), and images were processed in Adobe Photoshop CS6 (version 13.0).

2.9. Statistical analyses

The Chi-squared test for association was conducted for specimens resulting from treatment with dorsomorphin dihydrochloride. Larvae were scored and sorted into one of two categories: (1) embryos where all three body axes were detected, and (2) embryos with less than three axes. The Chi-squared test for association was used to determine if the ratio of larvae with and without all three axes was the same between dorsomorphin treatment at either the 4–32 cell stage or the 32–256 cell stage. An assumption necessary for conducting the chi-squared test for association dictates that there is variance. This assumption was not met in experimental conditions using SB431542 and DHM1.

3. Results

In *C. teleta,* the organizer cell 2d is born during the fourth cleavage division when the embryo contains 16 cells. Notably, cell 2d is much larger than other cells of the second quartet, making it easily identifiable (Fig. 1A, pseudo-colored in fuchsia). 2d extends deep inside the embryo, and as previously demonstrated by Amiel et al. (2013), it is in direct contact with the target cells that form head structures, specifically the 1st quartet micromere progeny $1a^1$, $1a^2$, $1b^1$, $1b^2$, $1c^1$, $1c^2$, $1d^1$, $1d^2$ (Fig. 1B–B′′).

Because 2d has direct contact with many cells in the embryo in *C. teleta*, we investigated the possibility that signaling between 2d and its target cells occurs via gap junction communication. Lucifer Yellow is a small compound that readily passes through gap junctions, and dye transfer to adjacent cells indicates functional gap junctions (Lee et al., 1987; Stewart, 1978). Previous studies in the mollusk *Patella vulgata* demonstrate gap junction communication among embryonic blastomeres at the stage when the D quadrant is specified and the dorsal-ventral axis is established (Damen and Dictus, 1996; de Laat et al., 1980; Dorresteijn et al., 1983). In these studies, Lucifer Yellow is rapidly transferred to adjacent cells following injection. In *C. teleta,* 2d was microinjected with Lucifer Yellow, and dye-coupling between 2d and other blastomeres was visually monitored for a minimum of 15 min, and often for the remainder of the cell cycle (up to 1 h). Spread of the Lucifer Yellow to adjacent cells is never observed ($n = 47$, four independent replicates) (Fig. 1C). Therefore, our analysis with Lucifer Yellow suggests that 2d does not signal to its immediate cell contacts via gap junctions. Instead, we hypothesize that cell 2d signals to its neighbors using paracrine signaling (Fig. 1D).

3.1. Inhibition experimental design

To determine whether the Activin/Nodal or BMP signaling pathway plays a role in organizing activity, experiments using small chemical inhibitors were conducted on *C. teleta* embryos during two independent time intervals at early cleavage stages (Fig. 2). The experimental time period is from the 4-cell stage to the 32-cell stage (4–32 cells), approximately 3 h. This time frame ensured that embryos were exposed to the inhibitory drug at two cleavage divisions prior to the birth of 2d, and remained in treatment until the 32 cell stage. By the 32 cell stage, cell 2d has divided and given rise to its daughter cells, $2d^1$ +

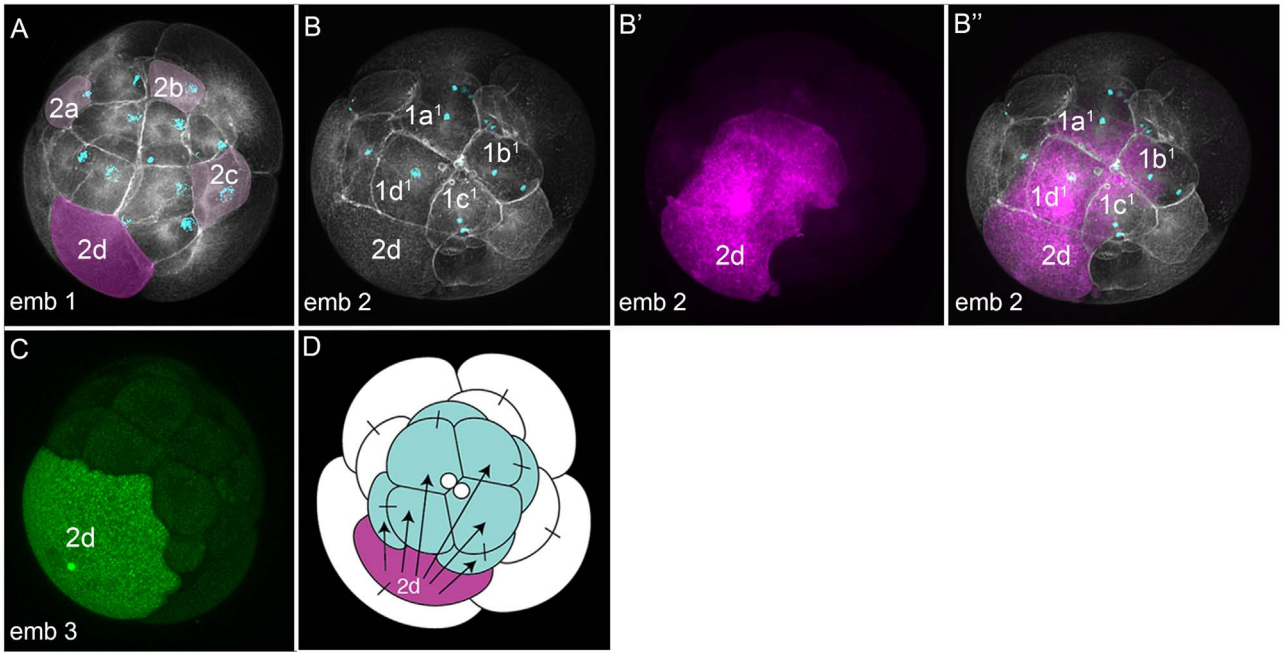

Fig. 1. Morphology and cell-cell contacts of 2d. A-C are z-stacks of merged confocal fluorescent images of 16 cell stage embryos in which the 2nd quartet has been born. In A, B, and B′′, cortical actin shows cell boundaries (white) and DNA is labeled in cyan by Hoechst staining. In C, green shows Lucifer Yellow. (A) Organizer cell 2d (pseudo colored in fuchsia) is the largest cell in the 2nd quartet. A second, different, embryo is depicted in B-B′′. (B) Embryo morphology, (B′) cell 2d microinjected and filled with red dextran, (B′′) merged image of B and B′ showing close spatial relationship between cell 2d and micromeres of the 1st quartet, $1a^1$, $1b^1$, $1c^1$, $1d^1$. (C) Cell 2d microinjected with Lucifer Yellow. (D) Diagram depicting the signaling activity of cell 2d (fuchsia) to cells of the 1st quartet (teal). emb 1, embryo 1; emb 2, embryo 2; emb 3, embryo 3.

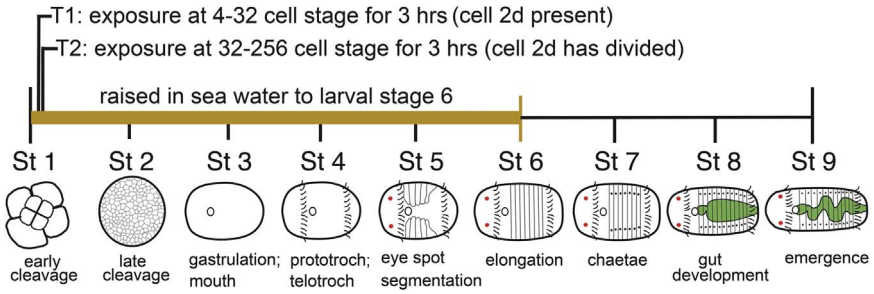

Fig. 2. Experimental design of drug exposure experiments. Diagram depicts the development of *Capitella teleta* from an early cleaving embryo through to late larval stages (stage 9). Each stage lasts approximately 24 h. The organizer cell, 2d, appears during early cleavage (stage 1). Drug exposures were conducted at two separate time points. At time point 1 (T1), chemical inhibitor was added to embryos at the 4 cell stage and removed at the 32 cell stage (approximately 3 h exposure). At time point 2 (T2), a chemical inhibitor was added to embryos at the 32 cell stage and removed at the 256 cell stage (approximately 3 h exposure). After the removal of the chemical inhibitor, embryos were raised in sea water to larval stage 6 (approximately 6 days) and analyzed phenotypically.

$2d^2$, and by this time, the organizer signal is no longer required for patterning of the head (Amiel et al., 2013). The control time interval is from the 32-cell stage to the 256-cell stage (32–256 cells) (approximately 3 h), which ensures that embryos are initially exposed to the drug after the requirement for organizing signal from 2d. Detailed phenotypic analysis was performed on larvae resulting from exposure to 40–50 μM SB431542 (Activin/Nodal inhibitor), 40 μM DMH1 (BMP inhibitor) or 5 μM dorsomorphin dihydrochloride (BMP inhibitor), as well as on control embryos exposed to a DMSO concentration equivalent to that of the experimental sample.

3.1.1. Activin/Nodal inhibition

Components of the Activin/Nodal signaling pathway are present in the *C. teleta* genome. SB431542 specifically targets ALK4, ALK5, and ALK7 Activin/Nodal type 1 receptors. Recent analyses describing the TGF-β signaling cassette in lophotrochozoans found that the *C. teleta* genome contains a single Activin/Nodal type 1 receptor ortholog of the *TGF-β Receptor I* (referred to here as *Ct-ALK4/5/7*) (Fig. 3A) (Kenny et al., 2014; Simakov et al., 2012). To assess the presence of receptor ALK4/5/7 as well as other downstream components necessary for Activin/Nodal signaling when the organizing signal is required, fluorescent *in situ* hybridization was conducted on embryos at the 16 cell stage (Fig. 3B-D′′). Expression of *Ct-ALK4/5/7* most often occurs in the micromeres of the 1st and 2nd quartet cells, and occasionally is detected in the macromeres (Fig. 3B-B′′). Similarly, *Ct-Activin Receptor 2 (Ct-ACVR2)* and *Ct-SMAD2/3*, the only type II receptor and receptor regulated SMAD specifically associated with Activin/Nodal signaling in the *C. teleta* genome, are often expressed in micromeres of the 1st and 2nd quartet cells (Fig. 3C-D′′) (Suppl. Table 1). For all three genes, expression is primarily associated with the nucleus with few cases of cytoplasmic expression. Although expression occurs in slightly varying patterns across specimens, this appears to correlate with the time of the cell cycle when the embryos were fixed. Altogether, this data reveals that components necessary for Activin/Nodal signaling are actively transcribed during the time-window when organizing activity is required in the embryo at the 16 cell stage. These observations support our hypothesis that SB431542 is in fact acting on the ALK4/5/7 receptor.

3.2. Axial properties of C. teleta larvae

C. teleta larvae conveniently have several morphological features that make identification of the anterior-posterior and dorsal-ventral axes, and bilateral symmetry straightforward (Fig. 4A-A′′′). Some identifiable anterior features include the brain, which can be visualized with nuclear staining (Fig. 4A′) and its position through the triangular arrangement of actin filaments circumventing the brain (Fig. 4A′′′) (Meyer and Seaver, 2009); presence of acetylated tubulin positive sensory cells (sc^{ac+}) along the dorsal edge of the brain (Fig. 4A′′); and an anterior ciliary band called the prototroch (Fig. 4A′′). Conversely, the posterior ciliary band, or telotroch, serves as a marker of posterior structures (Fig. 4A′′). Segmentally repeated circular muscles mark the position of the trunk (Fig. 4A′′′). When assessing the dorsal-ventral axis, identifiable ventral features include the mouth, which can be visualized as an opening or via nuclear staining and actin filament outlines (Fig. 4A′, A′′′); nuclear staining of the ganglia of the ventral nerve cord (Fig. 4A′); and a ventral ciliary band in the trunk called the neurotroch (Fig. 4A′′). Aside from the presence of sc^{ac+}, which are positioned on the dorsal edge of the brain (Fig. 4A′′), *C. teleta* lacks prominent morphological features on the dorsal side of the trunk. The presence of the ventrally occurring mouth, ventral nerve cord, and neurotroch on one side of the larva, coupled with the presence of dorsally positioned sc^{ac+} on the opposite side of the body serves to identify the dorsal-ventral axis. Identification of bilateral symmetry is possible when larvae are oriented ventrally (not shown) through the presence of features such as two symmetrical brain lobes, bilateral foregut anlagen, bilateral ventrolateral and dorsolateral longitudinal muscles (Fig. 4A′′′), and two laterally-positioned, symmetric larval eyes. The larval eye sensory cell has microvilli extending from its distal end that are visible via actin filament staining (Yamaguchi and Seaver, 2013).

Using these morphological features, we analyzed larvae exposed to 0.4% DMSO during the 4–32 cell stage (Fig. 4B-B′′′). These larvae are phenotypically normal and all three body axes are clearly evident (n = 279/291; n = 5 biological replicates). A subset of these larvae was further analyzed using Hoechst, phalloidin and acetylated tubulin (n = 50). In these, anterior features are present, including the brain (Fig. 4B′, B′′′), acetylated tubulin positive sensory cells (sc^{ac+}) along the dorsal edge of the brain (Figs. 4B′′ and 5A), and the prototroch (Fig. 4B′′). Trunk circumferential muscles and the posteriorly positioned telotroch are also present (Fig. 4B′′, B′′′). Together, these features confirm the presence of a clear anterior-posterior axis in 50/50 cases. Ventrally identifiable features include the mouth (Fig. 4B′′′), foregut, ventral nerve cord (Fig. 4B′), and the neurotroch (Fig. 4B′′). The presence of the sc^{ac+} that are positioned on the dorsal edge of the brain (Figs. 4B′′ and 5A) coupled with the presence of the ventrally occurring mouth, ventral nerve cord, and ventrally positioned neurotroch on the opposite axis, serve as an indicator of a clear dorsal-ventral axis in 48/50 cases (in n = 2/50 a neurotroch is not present, however all other dorsal-ventral features are present). Bilateral symmetry is also detectable via nuclear staining of the bilateral brain lobes (Fig. 5A), bilateral foregut anlagen, two larval eyes whose microvilli in the sensory cell can be seen with F-actin, and the presence of the two longitudinal actin filaments positioned on either side of the ventral midline (n = 50/50 cases) (Fig. 4B′′′). Larvae raised to stage 8, also posses chaetae, trunk specific structures (n = 7/7; data not shown).

Larvae resulting from exposure to 40 μM SB431542 during the 4–32 cell stage are phenotypically abnormal, but possess differentiated

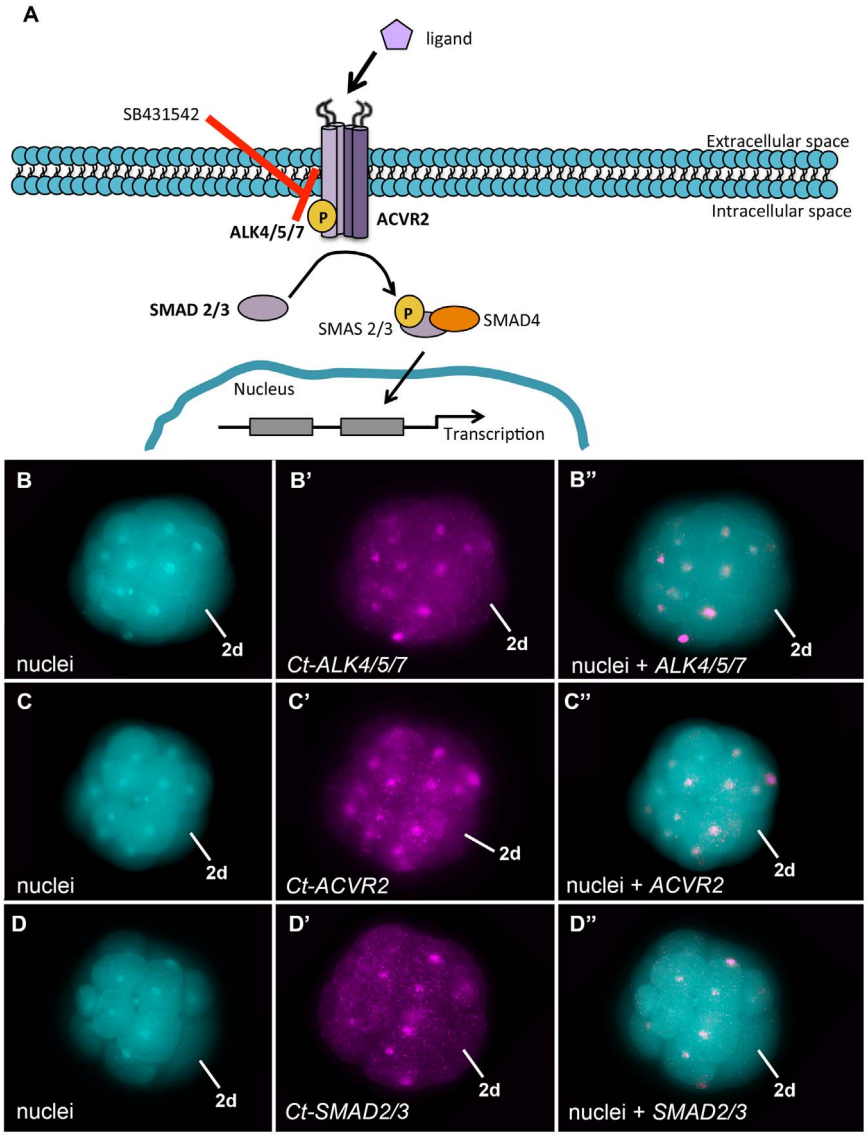

Fig. 3. Early expression of components in the Activin/Nodal pathway (A) Schematic depicts components of the Activin/Nodal signaling pathway and highlights inhibition of the phosphorylation of receptor ALK4/5/7 by the chemical inhibitor SB431542. (B-D'') 16 cell stage embryos. Images with the same letter correspond to images of a single embryo. (B, C, D) Merged confocal stack images labeled with anti-histone antibody to label nuclei. (B', C', D') Merged confocal stack images showing expression of *Ct-ALK4/5/7, Ct-Activin Receptor 2 (Ct-ACVR2),* and *Ct-SMAD2/3 by* fluorescent *in situ* hybridization. (B'', C'', D'') are merged confocal stack images of embryos labeled for both nuclei and gene expression.

cell types and polarity indicative of an anterior-posterior axis (Fig. 4C-C'''). Morphologically, in 346/443 cases (n = 7 biological replicates), larvae exhibit an abnormal spherical phenotype (Fig. 4C). Subsets of these larvae were further analyzed using Hoechst, phalloidin and an anti-acetylated tubulin antibody (n = 41). Larvae lack repeated circular muscle fibers, and although there are a few actin fibers, they are positionally disorganized (Fig. 4C''') (n = 40/41). In addition, larvae possess a single medial ciliary band that extends either completely or partly around the circumference of the larva (Fig. 4C'') (n = 40/41). It is not possible to morphologically distinguish whether this ciliary band is a prototroch or telotroch. The medial circumferential ciliary band was used as a landmark to orient the occurrence of any distinguishable features along an axis. An asymmetrically positioned ectodermal clearing is consistently observed on one end of the larvae (Fig. 4C). In untreated larvae, this ectodermal clearing is typically associated with early stages of the developing brain, although bilateral brain lobes are not detected in SB431542 treated animals when examined with a nuclear marker (Fig. 5D). In its place are disorganized small clusters of closely spaced nuclei positioned on the same end of the SB431542-treated animals as the ectodermal clearing (n = 40/41) (Figs. 4C, C' and 5D). Furthermore, when analyzed using anti-acetylated tubulin, acetylated tubulin-positive sensory cells (sc^{ac+}) are detected on the same end of the larvae as the ectodermal clearing, and are positioned within the clusters of closely spaced nuclei in 39/41 cases (in n = 2/41 sc^{ac+} were not detected) (Figs. 4C-C'' and 5D). In addition, chaetae, trunk specific structures that typically appear in stage 7 larvae, are not observed in any larvae raised for a longer period of time to stage 8 (n = 0/10; data not shown). Altogether, this information indicates the presence of an anterior identity on one end relative to the ciliary band, where there are features normally found in the head such as the ectodermal clearing, clusters of nuclei, and the sc^{ac+} (n = 39/41). In contrast, from analysis with these markers, there is no indication of trunk or posterior identity on the side of the ciliary band opposite the head.

A dorsal-ventral axis is indistinguishable in larvae resulting from exposure to 40 μM SB431542 during the 4–32 cell stage, since none of the larvae had ventral features such as the ventral nerve cord, neurotroch, or presence of a mouth (n = 0/41) (Fig. 4C'-C'''). Furthermore, the sc^{ac+} are positioned randomly, preventing the identification of dorsal identity (Fig. 5D). Bilateral symmetry is not

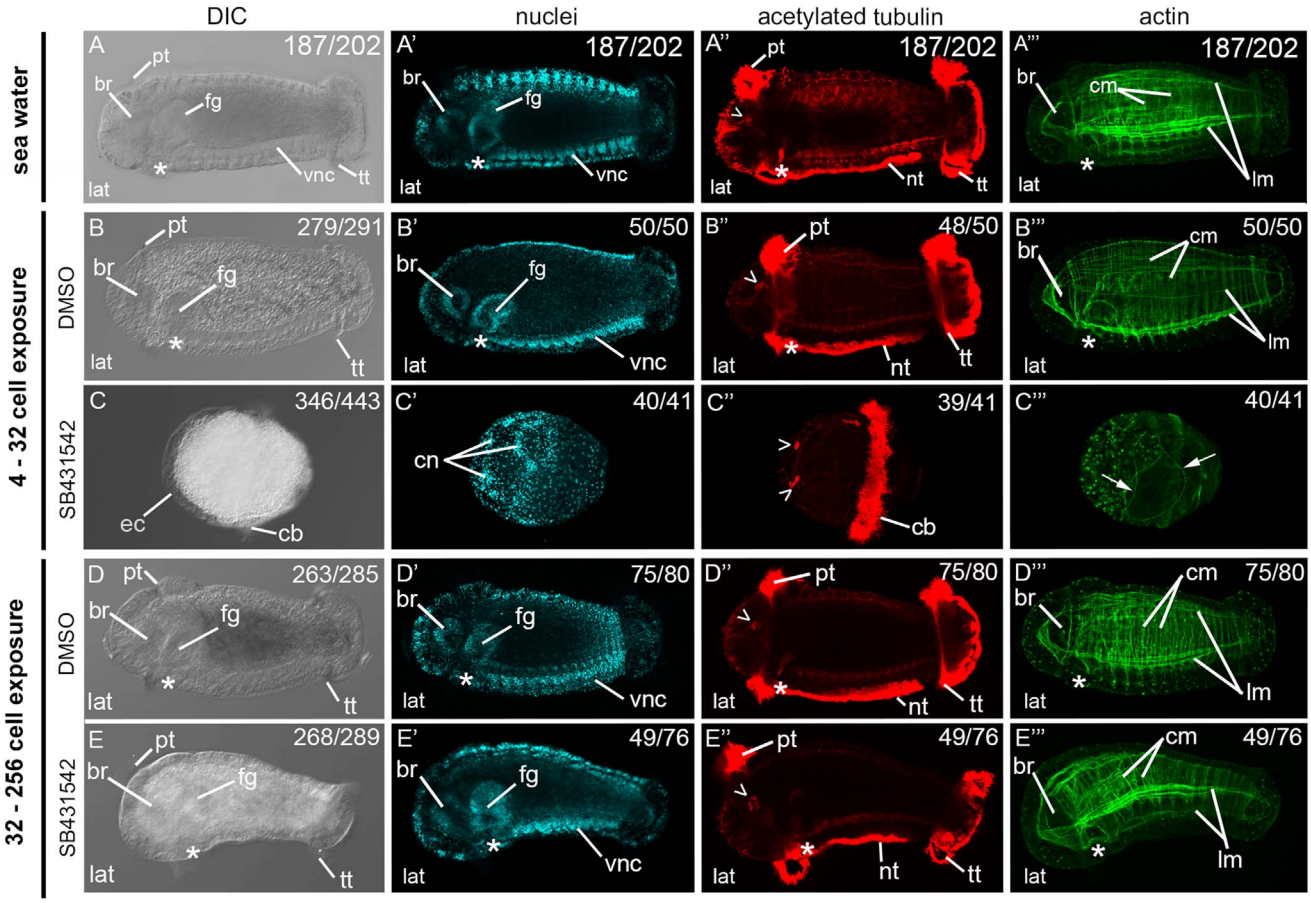

Fig. 4. Early exposure to SB431542 leads to abnormal larval morphology. Each row contains images of the same stage 6 larva raised in sea water or treated at a specified embryonic cell stage with either 0.4% DMSO as a control or 40 μM SB431542. Each column depicts either a DIC image (A-E) or merged confocal stack labeled for nuclei with Hoechst (A′- E′), cilia and neurons with anti-acetylated tubulin (A′′-E′′), or actin filaments with phalloidin (A′′′- E′′′). Images with the same letter correspond to images of a single animal. Figures A-A′′′ are images of a normal larva raised in sea water. Figures B-B′′′ are larvae treated with 0.4% DMSO during the 4–32 cell stage. Figures C-C′′′ are images of a larva treated with 40 μM SB431542 during the 4–32 cell stage. Figures D-D′′′ are images of control larvae treated with 0.4% DMSO during the 32–256 cell stage. Figures E-E′′′ are images of a larva treated with 40 μM SB431542 during the 32–256 cell stage. Open arrowhead, acetylated tubulin positive neurons; asterisk, position of the mouth; br, brain; cb, ciliary band; cm, circumferential muscle fibers; cn, clusters of nuclei; ec, ectodermal clearing; fg, foregut; lm, longitudinal muscle fibers; nt, neurotroch; pt, prototroch; tt, telotroch; vnc, ventral nerve cord.

detected due to the lack of bilateral brain lobes, lack of bilateral foregut anlage, randomly positioned sc^{ac+}, disorganized actin muscle fibers, and the absence of two eye spots (Figs. 4C′-C′′′ and 5D). Most larvae lack eyes entirely, but a few develop one to three eyes (data not shown).

To demonstrate the specificity of the phenotype resulting from inhibiting Activin/Nodal signaling, embryos were also exposed to 40 μM SB431542 between the 32 and 256 cell stage, a time frame after the signal from 2d has occurred. Larvae exposed to 0.4% DMSO during the 32–256 cell stage (Fig. 4D-D′′′) are morphologically normal (n = 263/285; n = 6 biological replicates). When a subset (n = 80) of these was further analyzed using Hoechst, phalloidin and an anti-acetylated tubulin antibody, all three body axes are distinguishable in 75/80 cases (in the remaining n = 5/80 cases, three axes were observed, however larvae were abnormally bent). Larvae resulting from exposure to 40 μM SB431542 during the 32–256 cell stage are morphologically elongated (n = 268/289; n = 6 biological replicates). When a subset (n = 76) of these elongated larvae was analyzed using Hoechst, phalloidin and an anti-acetylated tubulin antibody, all three body axes are detected (Fig. 4E-E′′′). Morphologically, in 27/76 cases, these larvae elongate normally along the anterior-posterior axis, but in 49/76 cases, the trunk is bent ventrally as is shown in Fig. 4E. Identifiable anterior features include the presence of a brain (Fig. 4E′, E′′′), acetylated tubulin-positive neurons in the head (Fig. 4E′′), prototroch (Fig. 4E′′), and two eyes. In the trunk, there are circumferential muscle fibers, and posteriorly, the telotroch is also present (Fig. 4E′′, E′′′). Together these features confirm the presence of a clear anterior-posterior axis (n = 76/76). Ventral features such as the mouth (Fig. 4E′′′), the ventral nerve cord (Fig. 4E′), and the neurotroch (Fig. 4E′′) are present. Acetylated tubulin-positive neurons in the head show a dorsal position (Figs. 4E′′ and 5G). Therefore, a clear dorsal-ventral axis is detected (n = 76/76). Bilateral symmetry is demonstrated by the presence of bilateral brain lobes, bilateral foregut anlage, two longitudinal actin filaments positioned on either side of the ventral midline, and two eyes (n = 76/76)(Fig. 5G). In summary, although not all the larvae resulting from treatment during the 32–256 cell stage are phenotypically normal, all three body axes are clearly present and there is normal patterning of head structures. Thus, exposure to the Activin/Nodal signaling inhibitor SB431542 during two different time intervals in early cleavage stages results in clear phenotypic differences in larvae.

3.3. *Ct-ADMP* expression is predominantly ventral

The *C. teleta* genome contains a single *ADMP* ortholog (Kenny et al., 2014), and we characterized its expression in hopes of using it as a ventral marker for the purpose of these experiments. Documentation of *Ct-ADMP* expression in larval stages reveals that expression predominantly occurs in the ectoderm along the ventral midline, and bilaterally in a subset of cells in both the foregut and trunk mesoderm (Suppl. Fig. S1). In early stage larvae (Stage 5), ectodermal expression

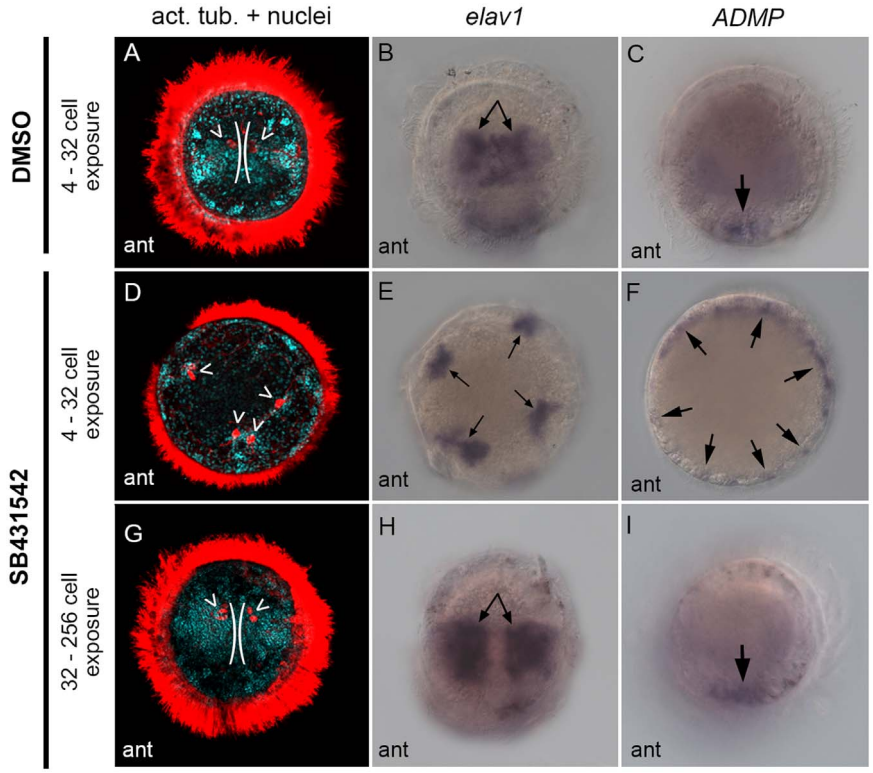

Fig. 5. Analysis of anterior features following exposure to SB431542. Each row contains images of a stage 6 larva in anterior view. Each column contains either a merged confocal stack image of larvae labeled for nuclei and acetylated tubulin or a DIC image depicting the expression of the axial markers, *CapI-elav1* and *Ct-ADMP*. Figures A-C are images of control larvae treated with 0.4% DMSO (a representative control phenotype). Figures D-F are images of larvae treated with 40 μM SB431542 during the 4–32 cell stage. Figures G-I are images of larvae treated with 40 μM SB431542 during the 32–256 cell stage. Arrowhead, acetylated tubulin positive sensory cells; black arrows, expression domains; white bracket, position of bilateral brain lobes.

is seen along the ventral midline (Suppl. Fig. S1A-A′′′). There is a small domain just anterior to the prototroch in the head (Suppl. Fig. S1A, A′′′), as well as ectodermal expression that extends the length of the trunk, starting posterior of the mouth and extending to the telotroch (Suppl. Fig. S1A-A′′′). Similarly, stage 6 (Suppl. Fig. S1B-B′′′), stage 7 (Suppl. Fig. S1C-C′′′), and stage 8 (Suppl. Fig. S1D-D′′′) larvae all possess expression along the midline of the ventral ectoderm, similar to that observed in stage 5 larvae. In these later stage larvae, two new expression domains appear in the mesoderm. The first is bilateral, and is positioned on either side of the foregut (white arrowheads). The second expression domain occurs as two distinct segmented bands in the trunk mesoderm, posterior to the foregut and anterior to the telotroch (white arrows; Suppl. Fig. S1B′, B′′′, C′, C′′′, D′, D′′′). The trunk mesoderm expression is localized to a lateral position and represents a subdomain of the trunk mesodermal tissue. In stage 9 larvae (Suppl. Fig. S1E-E′′′), ectodermal expression along the ventral midline becomes faint anterior to the prototroch, and is no longer detectable as a single expression domain along the entire length of the ventral trunk ectoderm (Suppl. Fig. S1E-E′′′). Expression associated with the foregut is in a narrow medio-lateral band (white arrowhead; Suppl. Fig. S1E′′′), and trunk mesodermal expression is no longer detectable. The *Ct-ADMP* expression pattern enables us to detect ventral ectoderm and lateral mesoderm in stage 6 larvae of SB431542 and DMSO-treated animals.

3.4. Inhibition of Activin/Nodal signaling in early embryos leads to abnormal expression of larval axial markers

Since we are unable to distinguish a dorsal-ventral axis or bilateral symmetry using Hoechst, phalloidin and acetylated tubulin in animals treated during the 4–32 cell stage, we continued our investigation into the presence of the three body axes and tissue differentiation by examining the expression of the following molecular markers by *in situ* hybridization: *CapI-elav1*, a marker of differentiating neurons that labels the bilateral brain and ventral nerve cord (Meyer and Seaver, 2009) (Figs. 5 and 6A); *CapI-foxA*, a foregut marker and indicator of bilateral symmetry and anterior trunk (Boyle and Seaver, 2008) (Fig. 6B); *Ct-ADMP*, a marker of ventral midline ectoderm, foregut, and lateral trunk mesoderm (Figs. 5 and 6C); *Ct-foxAB,* a marker of the ventrally positioned mouth and indicator of anterior trunk (Fig. 6D) (Boyle et al., 2014).

3.5. CapI-elav1

Larvae resulting from exposure to 0.4% DMSO in seawater during the 4–32 cell stage (n = 42/42), 0.4% DMSO in seawater during the 32–256 cell stage (n = 48/48; data not shown) or to 40 μM SB431542 during the 32–256 cell stage (n = 59/59) show characteristic expression domains for *CapI-elav1* (Fig. 6A, I). When viewed laterally, *CapI-elav1* expression is visible in the brain, indicating anterior, while expression within the trunk in the ventral nerve cord indicates ventral (Fig. 6A, I). When viewed anteriorly, *CapI-elav1* expression occurs in two large domains associated with the bilateral brain lobes, further indicating bilateral symmetry (Fig. 5B, H).

Examination of expression of *CapI-elav1* in larvae exposed to 40 μM SB431542 during the 4–32 cell stage reveals that a dorsal-ventral axis and bilateral symmetry are still indistinguishable. In 11/136 cases, *CapI-elav1* expression is not detectable. In 104/136 cases, *CapI-elav1* is expressed on the side of the ciliary band associated with anterior features such as the ectodermal clearing (Fig. 6E). The expression domains of *CapI-elav1*, which we believe to be cells with a neural identity, are randomly positioned (Fig. 5E), and are typically quite smaller than expression domains in the brains of controls (Fig. 5B). In the remaining 21/136 cases, there are two *elav1*

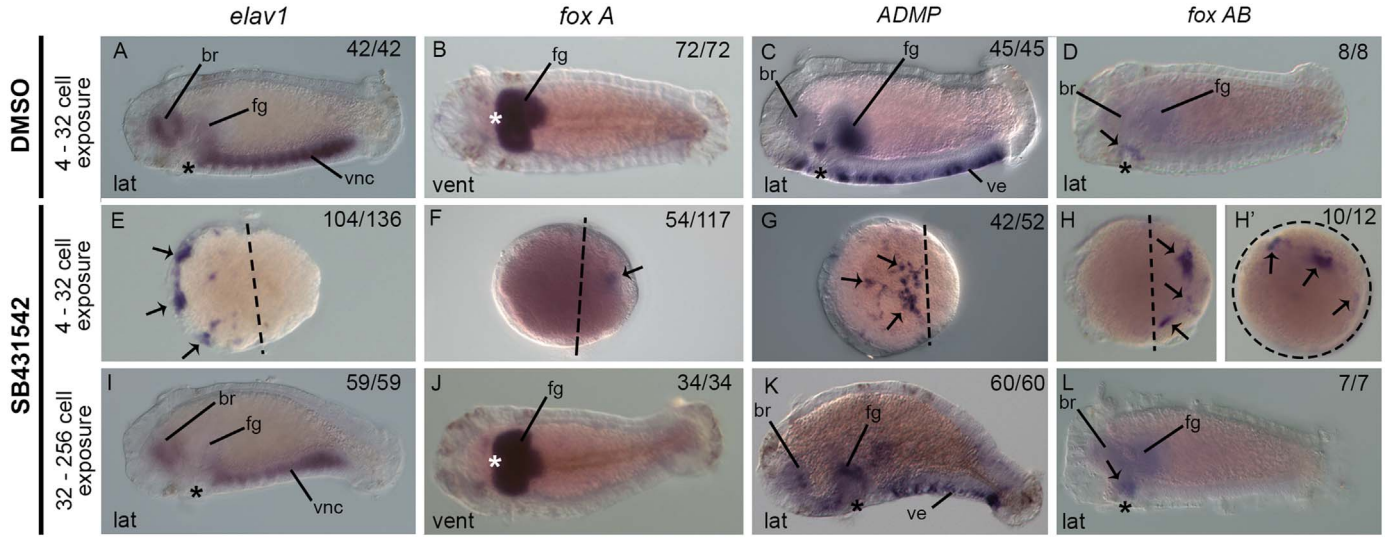

Fig. 6. Early exposure to SB431542 leads to abnormal expression of larval axial markers. Panels show expression of *CapI-elav1*, *CapI-foxA*, *Ct-ADMP*, and *Ct-fox AB* following *in situ* hybridization. A-D are larvae resulting from treatment with DMSO during the 4–32 cell stage (selected as a representative of control phenotype). E-H′ are larvae resulting from treatment with SB431542 during the 4–32 cell stage. I-L are larvae treated with SB431542 during the 32–256 cell stage. Specimens used to visualize *Ct-fox AB* expression were exposed to 50 μM SB431542 or 0.5% DMSO. All other specimens were exposed to 40 μM SB431542 or 0.4% DMSO. H & H′ are images of the same larva in different orientations (H, lateral view; H′ posterior view). All images are taken with DIC optics. Arrows indicate expression domains; asterisk indicates the position of the mouth; br, brain; dashed lines indicate position of ciliary band; fg, foregut; ve, ventral ectoderm; vnc, ventral nerve cord.

expression domains that could be interpreted as bilateral, although we do not have a definitive independent morphological landmark in these specimens for confirmation (data not shown). *CapI-elav1* expression is never seen on the posterior end of the larvae; thus, we are unable to detect ventral nervous system tissue in the trunk.

3.6. CapI-foxA

Larvae resulting from exposure to 0.4% DMSO in seawater during the 4–32 cell stage (n = 72/72), 0.4% DMSO in seawater during the 32–256 cell stage (n = 39/39; data not shown) or to 40 μM SB431542 during the 32–256 cell stage (n = 34/34), show characteristic bilateral expression of *CapI-foxA* in the foregut (Fig. 6B, J). In larvae exposed to 40 μM SB431542 during the 4–32 cell stage, *CapI-foxA* expression is not detectable in 63/117 cases. In the remaining 54/117 cases, *CapI-foxA* expression is detectable on the posterior side of the ciliary band; opposite the end with an ectodermal clearing (Fig. 6F). Although the *CapI-foxA* expression domain always occurs posterior to the ciliary band, its exact position varies. In some cases expression occurs immediately posterior to the ciliary band, in a central location, while in others expression is localized to the end of the animal. Additionally, the *CapI-foxA* expression domain is always substantially smaller than in controls, and is not bilateral (compare Fig. 6B, F).

3.7. Ct-ADMP

For embryos exposed to 0.4% DMSO in seawater during the 4–32 cell stage (n = 45/45), 0.4% DMSO in seawater during the 32–256 cell stage (n = 45/45; data not shown) or to 40 μM SB431542 during the 32–256 cell stage (n = 60/60), the resulting larvae show *Ct-ADMP* expression as expected in the ectoderm, mesoderm and foregut (Fig. 6C, K). In larvae exposed to 40 μM SB431542 during the 4–32 cell stage, there are 10/52 cases in which *Ct-ADMP* expression is not detectable. In the remaining 42/52 cases, ectodermal *Ct-ADMP* expression is detected on the side of the ciliary band associated with the ectodermal clearing (anterior end) (Fig. 6G). In control larvae and larvae resulting from exposure to 40 μM SB431542 during the 32–256 cell stage, the ectodermal *Ct-ADMP* expression domain anterior of the mouth and prototroch is small and localized to the ventral surface (Fig. 5C, I). However, for larvae resulting from treatment with 40 μM SB431542 during the 4–32 cell stage, the anterior expression domain is expanded around the circumference of the larva, indicating an expansion of ventral ectodermal identity anterior of the ciliary band (Fig. 5F, arrows). In addition, the lack of expression posterior to the ciliary band in the ectoderm, mesoderm and foregut may indicate a reduction in differentiation of trunk tissues (Fig. 6G).

3.8. Ct-foxAB

Larvae used to visualize *Ct-foxAB* expression were exposed to either 0.5% DMSO or 50 μM SB431542, a slightly higher concentration than otherwise described in this paper. However, as all resulting larvae exhibit similar phenotypes to those exposed to 40 μM SB431542, this data is also included here. Larvae resulting from exposure to 0.5% DMSO in seawater during the 4–32 cell stage (n = 8/8), 0.5% DMSO in seawater during the 32–256 cell stage (n = 10/10; data not shown) or to 50 μM SB431542 during the 32–256 cell stage (n = 7/7) show characteristic ventral expression of *Ct-foxAB* in the mouth (Fig. 6D, L). In larvae resulting from exposure to 50 μM SB431542 during the 4–32 cell stage, *Ct-foxAB* expression is not detectable in 2/12 cases. In the remaining 10/12 cases, *Ct-foxAB* expression is consistently detectable on the posterior side of the ciliary band; opposite the end with an ectodermal clearing (Fig. 6H-H′). Although *Ct-foxAB* expression always occurs posterior to the ciliary band, its exact size, position and number of distinct expression domains vary. The expression domains are randomly located on the posterior end, and therefore, a clear ventral side is not detectable. Furthermore, it is unlikely that *Ct-foxAB* expression indicates the presence of a mouth in these larvae as there are never any visible invaginations associated with the *Ct-foxAB* expression domains.

In summary, at the time in which the organizer cell 2d is active (4–32 cell stage), the inhibition of the Activin/Nodal signaling pathway results in larvae that possess anterior tissue identity on the side of the ciliary band associated with the ectodermal clearing. However, these data demonstrate that organization in the head is lost. There is also indication of a loss of trunk specification or differentiation of multiple cell types on the side opposite anterior (presumptive posterior). Taken together, we conclude that in animals treated during the 4–32 cell stage, an anterior-posterior axis is retained, but the dorsal-ventral axis and bilateral symmetry are lost.

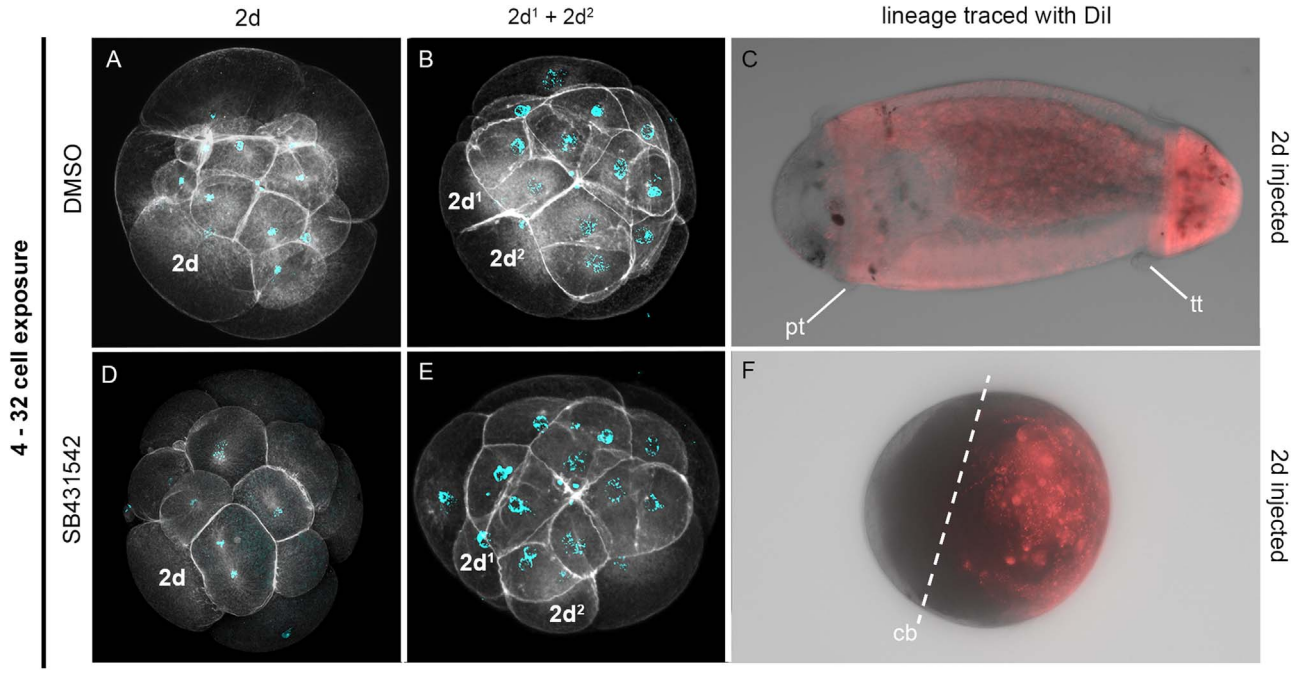

Fig. 7. Persistence of 2d lineage and its contribution to a reduced larval trunk Figures A-C depict control animals treated with 0.4% DMSO at the 4–32 cell stage. (A) Organizer cell 2d is the largest cell in the second quartet. (B) Daughter cells of 2d, $2d^1$ and $2d^2$. (C) Larva resulting from 2d microinjection with DiI showing trunk ectoderm and pygidium descendants (pink). Figures D-F depict animals treated with 40 μM SB431542 at the 4–32 cell stage. (D) In the presence of drug, cell 2d is born with its characteristic large size. (E) 2d daughter cells, $2d^1$ and $2d^2$ are born. (F) Larva resulting from 2d microinjection with DiI in drug treated animals. 2d generates a reduced trunk (pink). Larvae were imaged live in Figures C and F. Cb, ciliary band; cyan, nuclei; pt, prototroch; tt, telotroch; white, phalloidin labeling; white dotted line, ciliary band position.

3.9. Birth of cell 2d and its daughter cells $2d^1$ and $2d^2$ are not affected by SB431542 treatment, though its descendants contribute to a reduced larval trunk

Because the larval phenotype resulting from embryonic exposure to SB431542 bore striking similarities to embryos in which organizer cell 2d was deleted (Amiel et al., 2013), and there is reduction of trunk features, we were curious as to whether exposure to SB431542 prevented the birth of 2d or inhibited its subsequent development. To investigate this, embryos were exposed to either 0.4% DMSO as a control or 40 μM SB431542 during the 4 cell stage and monitored through two cleavage divisions to the 16 cell stage for the formation of the organizer cell 2d. In both control and SB431542 exposed embryos, cell 2d is born and has its characteristically large size, being the largest cell of the second quartet micromeres (Fig. 7A, D). Embryos were also monitored for another cleavage cycle, whereupon cell 2d divides and forms its daughter cells $2d^1$ and $2d^2$. In both control and SB431542 exposed embryos, 2d divides to produce daughter cells $2d^1$ and $2d^2$ in their characteristic positions (Meyer and Seaver, 2010) (Fig. 7B, E). These observations confirm that the formation and first division of 2d is unaffected in the presence of SB431542. To further investigate the development of 2d following exposure to SB431542 during the 4–32 cell stage, DiI was microinjected into 2d, and the embryos raised to larval stage 6 for analysis of labeled descendants. In control larvae exposed to 0.4% DMSO, descendants of 2d give rise to trunk ectoderm and pygidium as expected from a previous study describing the fate map of 2d (n = 12/12)(Fig. 7C) (Meyer et al., 2010). In animals treated with SB431542, the 2d lineage persists and contributes to the larva, but is abnormal (Fig. 7F). Although there is variation in the position of the boundary between labeled and unlabeled cells, the majority of the 2d descendant clone is positioned asymmetrically in the larva and is primarily localized to surface tissue on one side of the ciliary band, opposite the sc^{ac+} (n = 44/44) (Fig. 7F). This position is consistent with predictions from the 2d fate map. In 27/44 cases, small clusters of 2d descendant cells are also located on the side of the ciliary band where sc^{ac+} are present. Normally, the 2d lineage also contributes to a small portion of the left and right dorsal lobes of the brain, however, we have not confirmed if these labeled cells are neural in character (Meyer and Seaver, 2010). In 24/44 cases, we also saw small clusters of labeled cells in subsurface tissue; however, based on their appearance, we believe these to be sublineages that arrested during development.

In summary, the phenotypic similarities between larvae resulting from embryos in which 2d is deleted and those exposed to SB431542 during the 4–32 cell stage cannot be explained by a lack of 2d descendants via the death of 2d, an inability of 2d to produce its daughters $2d^1$ and $2d^2$, or a lack of contribution to the resulting larval body.

4. BMP inhibition

4.1. DMH1

DMH1 is a specific chemical inhibitor of ALK 2, a BMP type 1 receptor that phosphorylates SMAD 1/5/8, a BMP transcription factor (Hover et al., 2015). Recent analyses describing the TGF-β signaling cassette in lophotrochozoans found that the *C. teleta* genome contains *Activin Receptor 1* (also known as *ALK1/2)* and *SMAD 1/5/8* homologs (Kenny et al., 2014; Simakov et al., 2012). Larvae resulting from exposure to 40 μM DMH1 between the 4 and 32 cell stage do not possess any detectable abnormalities when examined morphologically, or with Hoechst, phalloidin and an anti-acetylated tubulin antibody (n = 119/119, three biological replicates; data not shown). A longer, 8 h exposure starting at the 32 cell stage also yields normal looking larvae (n = 40/40, two biological replicates; data not shown). As these exposures do not elicit any larval phenotypic effect, we are unable to confirm the efficacy of this drug in *C. teleta*.

4.2. Dorsomorphin dihydrochloride

Because we did not detect a phenotype when exposing embryos to DMH1, we elected to use a different BMP inhibiting drug, dorsomorphin dihydrochloride. Dorsomorphin functions by inhibiting the BMP

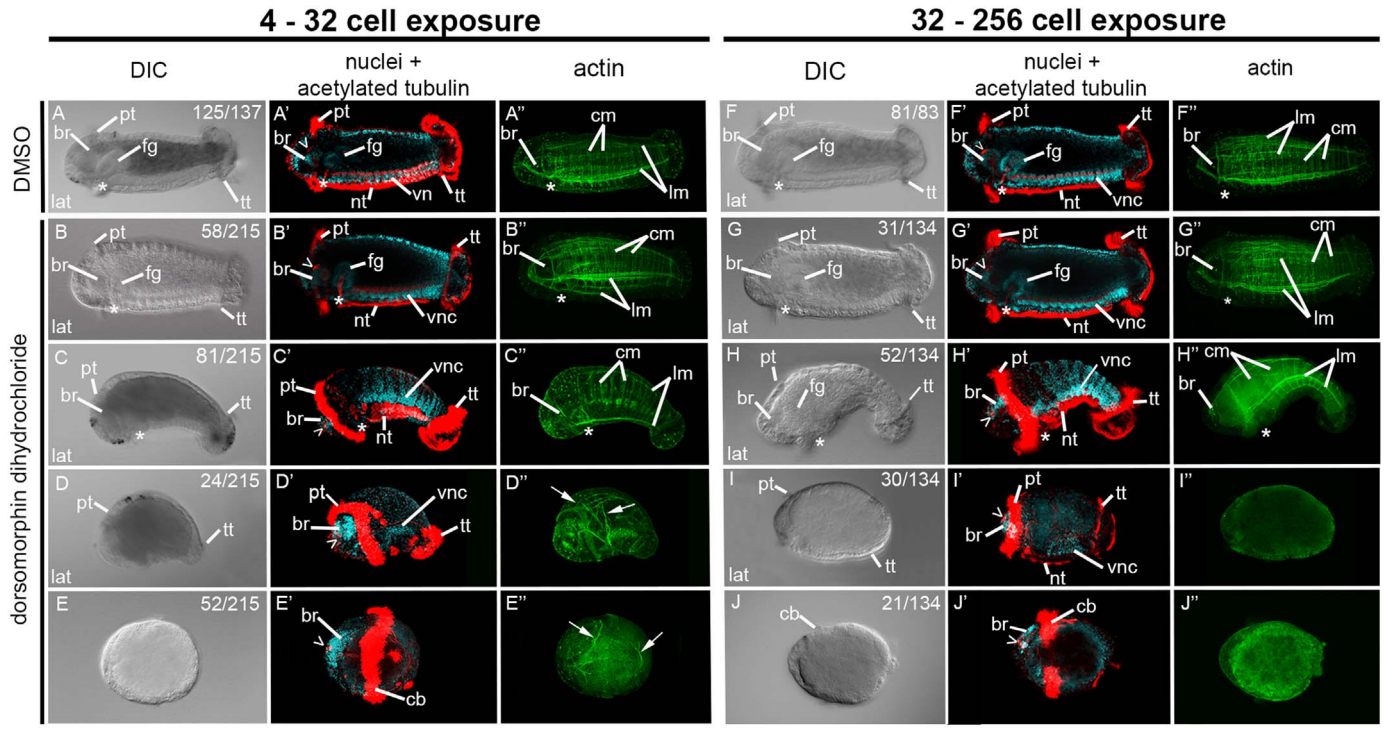

Fig. 8. Embryonic exposure to Dorsomorphin dihydrochloride results in a nonspecific phenotype. All images depict stage 6 larvae treated at a specified embryonic cell stage with either 0.05% DMSO as a control or 5 μM dorsomorphin dihydrochloride. Images with the same letter correspond to images of a single animal. Figures A-J viewed with DIC optics. Figures A′-J′ are combined channels of merged confocal stacks of larvae labeled for nuclei with Hoechst (cyan), and cilia and neurons with anti-acetylated tubulin (red). Figures A′′- E′′ and F′′-J′′ are single channel merged confocal stacks of larvae labeled for filamentous actin with phalloidin (green). Images in the first row depict control larvae treated with 0.05% DMSO during the 4–32 cell stage (A-A′′) or the 32–256 cell stage (F-F′′). Figures B-E′′ depict larval phenotypes produced when treated with 5 μM dorsomorphin dihydrochloride during the 4–32 cell stage. Figures G-J′′ depict larval phenotypes produced when treated with 5 μM dorsomorphin dihydrochloride during the 32–256 cell stage. br, brain; fg, foregut; asterisk, position of the mouth; vnc, ventral nerve cord; pt, prototroch; tt, telotroch; nt, neurotroch; arrowhead, acetylated tubulin positive sensory cells; cm, circumferential muscle; lm, longitudinal muscle; white arrow, actin filaments; cb, ciliary band.

type 1 receptors ALK 2 and ALK 3 (Anderson and Darshan, 2008). The *C. teleta* genome contains orthologs of both as *Activin Receptor 1* (also known as ALK1/2) and BMP Receptor 1 (also known as ALK3/6) (Kenny et al., 2014; Simakov et al., 2012). Embryos exposed to 0.05% DMSO during the 4–32 cell stage (Fig. 8A-A′′) result in phenotypically normal larvae in which all three body axes were distinguishable (n = 125/137; n = 4 biological replicates). In the remaining 12/137 cases, larvae possess slightly abnormal muscle organization. Analyses with Hoechst, phalloidin and an anti-acetylated tubulin antibody indicate that anterior features are present, including the brain (Fig. 8A′, A′′), sc^{ac+} along the dorsal edge of the brain (Fig. 8A′), and the presence of a prototroch (Fig. 8A′). The posteriorly occurring telotroch is also clearly visible (Fig. 8A′). Together these features confirm the presence of a clear anterior-posterior axis in 125/137 cases. Ventral features such as the mouth, foregut, ventral nerve cord, and the neurotroch, along with the sc^{ac+} on the dorsal edge of the brain are all visible, demonstrating the presence of a dorsal-ventral axis in 125/137 cases (Fig. 8A′, A′′). Bilateral symmetry is also detected through the presence of a bilateral brain, bilateral foregut, two larval eyes, and the presence of the two longitudinal muscle fibers positioned on either side of the ventral midline in 125/137 cases.

Embryos exposed to 5 μM dorsomorphin dihydrochloride during the 4–32 cell stage result in four reproducible and distinct larval phenotypes: normal larvae (n = 58/215; n = 4 biological replicates) (Fig. 8B-B′′); ventrally bent larvae (n = 81/215) (Fig. 8C′-C′′); partially elongated larvae (n = 24/215) (Fig. 8D-D′′); and non-elongated larvae (n = 52/215) (Fig. 8E-E′′). When analyzed with Hoechst, phalloidin and an anti-acetylated tubulin antibody, normal larvae (Fig. 8B′-B′′), ventrally bent larvae (Fig. 8C′-C′′), and partially elongated larvae (Fig. 8D′-D′′) all possess anterior features such as the brain, sc^{ac+} along the dorsal edge of the brain, and the prototroch. The posterior telotroch is also present. Together these features confirm the presence of a clear anterior-posterior axis in 163/215 cases. Ventral features are also present in the normal (Fig. 8B′-B′′) and ventrally bent (Fig. 8C′-C′′) larvae, including the mouth, the ventral nerve cord, and neurotroch. In the partially elongated larvae, there is no detectable invagination or developing foregut tissue (visible by Hoechst and transmitted light microscopy) to indicate presence of a mouth or foregut (Fig. 8D, D′). There is also a significant reduction in the number of actin fibers, and the fibers present are highly disorganized (Fig. 8D′′). However, the presence of both a partial ventral nerve cord and partial neurotroch show the presence of ventral identity (Fig. 8D′). In both the ventrally bent (Fig. 8C′) and partially elongated (Fig. 8D′) larvae, a foregut is not detectable. Altogether, the presence of sc^{ac+} coupled with the presence of the ventral nerve cord and neurotroch on the opposite side of the body in the normal (Fig. 8B′), ventrally bent (Fig. 8C′), and partially elongated (Fig. 8D′) larvae, indicates a clear dorsal-ventral axis in 163/215 cases. In the normal (Fig. 8B′-B′′) and ventrally bent (Fig. 8C′-C′′) larvae, bilateral symmetry is also detected through the presence of a bilateral brain, longitudinal actin filaments positioned on either side of the ventral midline, as well as two larval eyes detected with phalloidin staining (not shown). In the partially elongated larvae (Fig. 8D′-D′′), bilateral symmetry is discerned through the presence of bilateral brain lobes. Overall, in three out of the four observed phenotypes, there are anterior-posterior and dorsal-ventral axes, and bilateral symmetry is detectable (n = 163/215).

In non-elongated larvae (Fig. 8E-E′′), anterior features such as the brain, visible as tight clustering of nuclei relative to the surrounding tissue (Fig. 8E′), and the sc^{ac+} are present (Fig. 8E′). These larvae lack repeated circular muscle fibers, and although there are a few actin fibers, they are positionally disorganized (Fig. 8E′′). There are no visible invaginations to indicate a mouth, or foregut tissue or actin

fibers that characteristically surround the mouth. Furthermore, there is no clear prototroch or telotroch, as these larvae only possess a single ciliary band that is either circumferential or semi-circumferential, and occurs near the middle of the larvae (Fig. 8E′). Altogether, this information indicates anterior identity whereby on one end relative to the ciliary band, there exist features normally found in the head such as the brain and the sc^{ac+}. There is no indication of a trunk or posterior identity on the side of the larva opposite the head features. A dorsal-ventral axis is indistinguishable since all ventral features scored, such as the mouth, the ventral nerve cord, and the neurotroch are missing (n = 52/52) (Fig. 8E′-E′′). Bilateral symmetry is not detected due to the lack of bilateral brain lobes, lack of bilateral foregut anlage, positionally disorganized actin muscle fibers, and the absence of two eyes (Fig. 8E′-E′′). Thus in 52/215 cases, anterior polarity is detected, but dorsal-ventral and bilateral symmetry are indistinguishable. Altogether, in three out of four phenotypes, there are anterior-posterior and dorsal-ventral axes, and bilateral symmetry is detectable (n = 163/215).

To assess the specificity of the phenotype resulting from inhibiting BMP signaling during organizing activity, embryos were exposed to 5 μM dorsomorphin dihydrochloride during the 32–256 cell stage, a time interval after the signal from 2d has occurred. Larvae resulting from exposure to 0.05% DMSO during the 32–256 cell stage are phenotypically normal (n = 81/83; n = 3 biological replicates), and when analyzed with Hoechst, phalloidin and anti-acetylated tubulin, all three body axes are clearly distinguishable (Fig. 8F-F′′).

Embryos exposed to 5 μM dorsomorphin dihydrochloride during the 32–256 cell stage (n = 3 biological replicates) results in four larval phenotypes, all of which bear the same morphological features and axial properties as the four phenotypes produced following exposure during the 4–32 cell stage: normal larvae (n = 31/134) (Fig. 8G-G′′); ventrally bent larvae (n = 52/134) (Fig. 8H-H′′); partially elongated larvae (n = 30/134) (Fig. 8I-I′′); and non-elongated larvae (n = 21/134) (Fig. 8J-J′′). Minor differences do exist between the phenotypes of the 32–256 cell stage versus the 4–32 cell stage exposure time intervals. For instance, partially elongated (Fig. 8I′′), and non-elongated larvae (Fig. 8J′′) resulting from exposure during the 32–256 cell stage have no detectable actin muscle fibers, while a small number of disorganized muscle fibers are detectable in partially elongated and non-elongated larvae resulting from embryos treated during the 4–32 cell stages (Fig. 8D′′, E′′). While there is indication of anterior polarity in non-elongated larvae, a dorsal-ventral axis and bilateral symmetry were not detected (n = 21/134). Altogether, in three out of four phenotypes, there are anterior-posterior and dorsal-ventral axes, and bilateral symmetry is detectable (n = 113/134).

Since the phenotypes produced from embryonic exposure during the 4–32 cell stage are similar to that seen during the 32–256 cell stages, a chi-square test was conducted for association between time period of exposure and presence of axes. The results of this test indicate that there is no significant difference between the ratio of larvae with and without all three body axes resulting from exposure between the 4–32 and the 32–256 stages (chi-squared test, x^2 (1) = 5.195, df = 1, P = 0.057). Valuation of the effect size (Phi test, φ = −0.102, P = 0.057) reveals a small effect size. Altogether, this supports the interpretation that there is no difference in the proportions of larvae with and without all three body axes between the two time periods. These data indicate that the resulting phenotypes are not the product of organizing activity.

5. Discussion

5.1. ADMP as a ventral marker

In this study, *Ct-ADMP* functions as a key marker to identify ventral identity in *C. teleta* larvae, since it is expressed in a band of ventral ectodermal cells in the head and trunk. *ADMP* expression is also associated with ventral identity in several developing bilaterian animals. For instance, in the echinoderm *Strongylocentrotus purpuratus* and in the hemichordate *Saccoglossus kowalevskii*, *ADMP* expression is detected during late gastrula stages both along the ventral midline of the ectoderm and in portions of the ventral endoderm (Chang et al., 2016; Lowe et al., 2006). Likewise, in the planarian *Schmidtea mediterranea* and the acoel flatworm *Hofstenia miamia, ADMP* expression is both detected in sub-epidermal cells along the ventral midline and laterally along the dorsal-ventral boundary in adults (Gaviño and Reddien, 2011; Molina et al., 2011; Srivastava et al., 2014). In annelids, documentation of *ADMP* expression is limited (Boilly et al., 2017). In the clitellate annelid *Helobdella robusta*, embryonic *ADMP* expression is broad throughout the germinal bands and does not appear to be localized to the ventral side (Kuo and Weisblat, 2011). In *C. teleta* larvae, the ventral ectoderm expression of *Ct-ADMP* is conserved with that of planarians, acoels, hemichordates and sea urchins, occurring along the ventral midline ectoderm, making *Ct-ADMP* an ideal ventral marker for detection of axes.

5.2. The Activin/Nodal pathway is essential for establishing the dorsal-ventral axis and specification of trunk identity

The small molecule inhibitor SB431542 was used to interfere with the activation of the Activin/Nodal signaling pathway in *C. teleta* embryos. SB431542 functions by preventing the phosphorylation of type 1 receptors ALK4, ALK5, and ALK7 in the Activin/Nodal signaling pathway (Inman et al., 2002). In the *C. teleta* genome, there are only three type 1 receptors belonging to the TGF-β superfamily. These are *ALK1/2*, and *ALK3/6*, which are associated with BMP signaling, and *ALK4/5/7*, which is associated with Activin/Nodal signaling (Kenny et al., 2014; Simakov et al., 2012). Accordingly, SB431542 is likely acting upon the ALK4/5/7 receptor, the presence of which we show at 16 cell stage.

Inhibition of signaling via the ALK4/5/7 receptor by SB431542 during the 4–32 cell stage in *C. teleta* produce larvae that retain an anterior-posterior axis but lack a clear dorsal-ventral axis and bilateral symmetry. Interestingly, this is not the case for drug exposure experiments during the 32–256 cell stage, as those resulting larvae retained anterior-posterior, dorsal-ventral axes, and bilateral symmetry. As such, the larval phenotype resulting from SB431542 exposure during the 4–32 cell stage is likely the result of inhibiting the activity of the organizer signal since the effect is restricted to the time window during which organizing activity occurs. We further observe that in animals treated with SB431542 during the 4–32 cell stage, the head becomes ventralized. Specifically, *Ct-ADMP* expression is in a broad circumferential pattern in the head ectoderm, indicative of an expansion of ventral identity. In the hemichordate *S. kowalevskii*, a similar radial expansion of anterior *ADMP* expression is seen following the knockdown of *BMP2/4*, a dorsal patterning gene (Lowe et al., 2006). Likewise, in *C. teleta,* signaling via the ALK4/5/7 receptor appears to be essential for dorsal patterning.

In *C. teleta,* our results indicate that the patterning of the anterior-posterior axis is uncoupled from that of dorsal-ventral and bilateral symmetry. Although treatment with SB431542 during the 4–32 cell stage results in radialized larvae, the medial ciliary band acts as a boundary that enabled us to detect the polarization of several features and distinguish clear anterior and posterior ends. Since the inhibition of the ALK4/5/7 receptor with SB431542 during organizing activity affects patterning of the dorsal-ventral axis and bilateral symmetry, but not the anterior-posterior axis, the formation of the anterior-posterior axis is likely dependent on a different signaling pathway and/or occurs during a different time window. It is likely that the anterior-posterior axis is patterned prior to organizing activity, although this has not yet been directly investigated in *C. teleta*. In some bilaterians, the specification of the anterior-posterior axis is separate from the specification of the dorsal-ventral axis (Goldstein and Freeman, 1997). For example, in most sea urchins (echinoderms) and snails (mollusks), the anterior-posterior axis corresponds to the animal-

vegetal axis in the zygote and is specified during oogenesis, while the dorsal-ventral axis is specified later, after fertilization (Goldstein and Freeman, 1997; Guerrier et al., 1978; Henry et al., 1992; Lartillot et al., 2002). In contrast, in chordates like *Xenopus*, specification of the anterior-posterior, dorsal-ventral, and left-right axes all occur during gastrulation via signals from the organizer (Gerhart et al., 1989; Spemann and Mangold, 1924; Yamaguchi, 2001).

One unexpected finding from inhibition of ALK4/5/7 with SB431542 during the 4–32 cell stage is that there is loss of most trunk features. This result suggests that there is a lack of specification or differentiation of trunk identity. Through lineage tracing of 2d in drug treated embryos, we demonstrated that the 2d lineage contributes to these larvae, and we determined which half of the radialized larvae, relative to the medial ciliary band, is the presumptive trunk. We were further able to eliminate the possibility that 2d is not born, or that the 2d lineage arrests immediately following drug exposure, a concern due to the striking phenotypic similarities between drug treated and 2d laser deleted animals (Amiel et al., 2013). One explanation that may account for the phenotypic similarities seen between 2d-deleted and drug-treated animals is that organizing activity is also crucial for specifying the fate of cell 2d itself. Since descendants of 2d do not generate all of the ectoderm on the posterior side of drug treated larvae, the possibility exists that in the absence of an organizing signal, other cell(s) also contribute to trunk ectoderm. Thus when 2d is deleted, these unidentified cells compensate for the ectoderm. Likewise, when organizing signal is chemically inhibited, the fate of 2d is affected, thus both 2d and these unidentified compensatory cells generate trunk ectoderm.

Furthermore, our analysis reveals loss of expression of several markers and structures in the trunk of larvae resulting from embryos exposed to SB431542 during the 4–32 cell stage. For instance, although there is detectable *Ct-ADMP* and *CapI-elav1* expression in the anterior region of the larva resulting from drug treatment, expression of both genes is absent from the trunk. Also absent are chaetae and circumferential muscle fibers, both of which are trunk-specific structures. Markers that are expressed in the trunk are *Ct-foxAB*, a mouth marker in *C. teleta*, and expression of *CapI-foxA* in a little less than half of the cases. Expression is not completely normal for either gene however. One explanation for the observed multiple domains of expression is that the *Ct-foxAB*-expressing cells may fail to undergo normal migration and coalesce into a single structure. Altogether, our data suggests that there has been a reduction in the differentiation or specification of the larval trunk, including in neural, non-neural ectoderm and mesodermal structures.

The *C. teleta* genome contains several *activin/inhibin/myostatin-like* genes and *nodal*, Activin/Nodal branch ligands that might function via binding to the ALK4/5/7 receptor (Kenny et al., 2014; Simakov et al., 2012). It is tantalizing to think that nodal is in fact the organizing activity signal since it plays an essential role in patterning the dorsal-ventral, left-right, and in some cases the anterior-posterior axes for a range of bilaterians. For example, nodal is crucial for dorsal-ventral patterning in the hemichordate *Ptychodera flava* (Rottinger et al., 2015); for left-right patterning in the mollusks *Biomphalaria glabrata* and *Lottia gigantea* (Grande and Patel, 2009); dorsal-ventral and left-right patterning in the echinoderm sea urchin (Duboc et al., 2005, 2004; Lapraz et al., 2015; Molina et al., 2013); and for dorsal-ventral, left-right, and anterior-posterior patterning in chordates such as mouse, zebrafish, and *Xenopus*, (Brennan et al., 2001; Schier and Shen, 2000; Shen, 2007). However, until directly tested functionally, it must be considered that any one of the aforementioned ligands may function via the ALK4/5/7 receptor.

In summary, our data suggests that in *C. teleta*, signaling via the ALK4/5/7 receptor patterns the dorsal-ventral axis and bilateral symmetry, implicating the Activin/Nodal pathway as having a role in *C. teleta* organizing activity. It is likely that 2d is emitting an Activin/Nodal class ligand to surrounding cells, including to the 1st quartet micromeres, and thus patterning dorsal-ventral and bilateral symmetry. However, because of the nature of our experimental design, it is also possible that 2d responds to Activin/Nodal class ligands emitted by neighboring cells by turning on a second, downstream signal that effectively patterns the dorsal-ventral axis. If such is the case, it is unlikely that cells 2D or those of the 1st quartet play a role in activating downstream signaling in 2d. Previous deletion studies demonstrated that the removal of cell 2D (the sister cell of 2d) or of 1a + 1b + 1c + 1d (all of the first quartet micromeres) does not affect dorsal-ventral axis patterning (Amiel et al., 2013; Yamaguchi et al., 2016). Altogether, it is clear that signaling via the ALK4/5/7 receptor plays a crucial role be it direct or indirect, in patterning the dorsal-ventral axis and bilateral symmetry in *C. teleta*.

5.3. Role of BMP in patterning the dorsal-ventral axis in other spiralians

Recent studies in a few spiralian species have suggested that BMPs play a crucial role in patterning along the dorsal-ventral axis (Kuo and Weisblat, 2011; Lambert et al., 2016; Tan et al., 2017). A study conducted on the mollusk, *Crassostrea gigas,* found *BMP2-4* expression to be localized to cells on the dorsal side of the embryo, and that expression of the BMP antagonist *Chordin* is localized to cells on the ventral side of the embryo (Tan et al., 2017). The researchers argue that these complementary expression patterns suggests an antagonistic relationship between *BMP2-4* and *Chordin* in patterning the dorsal-ventral axis in *C. gigas* (Tan et al., 2017). Similarly, in the gastropod mollusk, *Ilyanassa obsoleta*, mRNA expression patterns indicate that *BMP2-4* is most strongly expressed on the dorsal side of the embryo, in the organizer cell 3D and its neighbors (Lambert et al., 2016). Knockdown of *BMP2-4* using morpholinos results in radialized animals that are phenotypically similar to embryos in which the organizer is ablated via polar lobe removal. The polar lobe is a transient protrusion that forms during the first few cell divisions in spiralians, and contains cytoplasmic determinants that are specifically shunted into the CD and D blastomeres (Clement, 1952). The addition of recombinant BMP4 ligand following polar lobe removal in *I. obsoleta* results in the recovery of structures normally distributed along the dorsal-ventral axis, providing experimental evidence that BMP2-4 is essential for dorsal-ventral patterning in this mollusk (Lambert et al., 2016).

The results from molluscan embryos contrast with *BMP* expression and function in the annelid *Helobdella robusta* (Kuo and Weisblat, 2011). Whereas *BMP2-4* expression is localized to the dorsal side of the aforementioned molluscan embryos, in *Helobdella, BMP2-4* genes are broadly expressed. Rather, it is *BMP5-8* that is specifically expressed on the dorsal side of the embryo. Furthermore, it is gremlin, not chordin, that promotes ventral cell fates, though its expression domain also includes the dorsal side of the embryo. Knockdown experiments using morpholinos demonstrate that BMP5-8 specifies dorsal cell fates, while gremlin functions by antagonizing the broadly expressed BMPs, but not the dorsally expressed BMP5-8 (Kuo and Weisblat, 2011). Altogether, these studies suggest that in other spiralians, BMP signaling plays an essential role in dorsal-ventral axis formation. Furthermore, there appears to be species variation in the molecular details of which components of the pathway are utilized, particularly ligands and antagonists, and how these components interact with each other in a functional signaling pathway.

5.4. BMP signaling is not implicated in organizing activity in C. teleta

In this study, we find no direct evidence to suggest that BMP signaling plays a role in axes formation in *C. teleta*. Although DMH1 has demonstrable effects on BMP signaling in chordates, hemichordates, and brachiopods (Chang et al., 2016; Hao et al., 2011; Martín-Durán et al., 2016), we are unable to detect any developmental defects in *C. teleta* larvae even after extended exposure with the drug. This

suggests that DMH1 may be ineffective in *C. teleta*. We also used another less specific BMP chemical inhibitor, dorsomorphin (Anderson and Darshan, 2008; Arrowsmith et al., 2015; Vogt et al., 2011). Dorsomorphin does not specifically inhibit organizing activity in *C. teleta*. Embryos exposed to dorsomorphin either during the time of organizing activity or during a later time frame result in similar larval phenotypes that are not significantly different between the two time periods. Since embryonic organizing activity ends at the 16 cell stage, following the division of cell 2d (Amiel et al., 2013), if dorsomorphin did inhibit the organizing activity signal, axially abnormal larvae would be restricted to treatments during the 4–32 cell stage. As such, while dorsomorphin clearly has an effect on larval development in *C. teleta*, it is not a result of inhibiting the organizer activity signal. Although BMP signaling is not the organizing signal, this pathway may still play a role in early development. It is probable that the Activin/Nodal organizing signal activates downstream BMP signaling, which is crucial for larval development. Interestingly however, the application of exogenous BMP4 protein during early cleavage stages in *C. teleta* does not appear to affect dorsal-ventral patterning (Corbet et al., 2018).

As there are differences between taxa as to which TGF-β superfamily ligands function in axis formation, it may not be entirely surprising to find that *C. teleta* represents a slightly more dramatic example of this variation by utilizing ligands from the Activin/Nodal signaling pathway for organizing activity, rather than from the BMP pathway. It is intriguing to note that in the two annelids in which dorsal-ventral patterning has been examined, the molecular identity of the TGF-β superfamily components of the pathway that are utilized for dorsal-ventral patterning differ from those used in mollusks.

In summary, our data supports the idea that in *C. teleta,* signaling via the ALK4/5/7 receptor patterns the dorsal-ventral axis and bilateral symmetry, implicating the Activin/Nodal pathway as the *C. teleta* organizing activity signal. Future functional genomic studies are needed in order to decipher which Activin/Nodal class ligand is activating the organizing activity of the signaling pathway, and to confirm that the signal is transmitted via the ALK4/5 receptor. Furthermore, in this study we confirm that in *C. teleta,* the formation of the anterior-posterior axis is uncoupled from the formation of the dorsal-ventral axis and bilateral symmetry. Finally, our findings highlight differences among spiralians in how the molecular components of the conserved TGF-β superfamily signaling pathway are utilized to mediate patterning of the dorsal-ventral axis and bilateral symmetry during early spiralian development.

Acknowledgements

We thank Dr. Kariena K. Dill for cloning the *Ct-ADMP* and *Ct-SMAD2/3* genes, Dr. Marleen Klann for optimizing the fluorescent *in situ* protocol in *C. teleta*, Sondre Skarsten for assistance with statistical analysis, and Dr. Danielle de Jong, Dr. Marleen Klann and Leah Dannenberg for useful comments on the manuscript. This work was supported by the National Science Foundation (IOS1457102 to ECS).

Appendix A. Supporting information

Supplementary data associated with this article can be found in the online version at doi:10.1016/j.ydbio.2018.01.004.

References

Ackermann, C., Dorresteijn, A., Fischer, A., 2005. Clonal domains in postlarval *Platynereis dumerilii* (Annelida: polychaeta). J. Morphol. 266, 258–280. http://dx.doi.org/10.1002/jmor.10375.

Amiel, A.R., Henry, J.Q., Seaver, E.C., 2013. An organizing activity is required for head patterning and cell fate specification in the polychaete annelid *Capitella teleta*: new insights into cell-cell signaling in Lophotrochozoa. Dev. Biol. 379, 107–122. http://dx.doi.org/10.1016/j.ydbio.2013.04.011.

Anderson, G.J., Darshan, D., 2008. Small-molecule dissection of BMP signaling. Nat. Chem. Biol. 4, 15–16. http://dx.doi.org/10.1038/nchembio0108-15.

Arrowsmith, C.H., Audia, J.E., Austin, C., Baell, J., Bennett, J., Blagg, J., Bountra, C., Brennan, P.E., Brown, P.J., Bunnage, M.E., Buser-Doepner, C., Campbell, R.M., Carter, A.J., Cohen, P., Copeland, R.A., Cravatt, B., Dahlin, J.L., Dhanak, D., Edwards, A.M., Frederiksen, M., Frye, S.V., Gray, N., Grimshaw, C.E., Hepworth, D., Howe, T., Huber, K.V.M., Jin, J., Knapp, S., Kotz, J.D., Kruger, R.G., Lowe, D., Mader, M.M., Marsden, B., Mueller-Fahrnow, A., Müller, S., O'Hagan, R.C., Overington, J.P., Owen, D.R., Rosenberg, S.H., Ross, R., Roth, B., Schapira, M., Schreiber, S.L., Shoichet, B., Sundström, M., Superti-Furga, G., Taunton, J., Toledo-Sherman, L., Walpole, C., Walters, M.A., Willson, T.M., Workman, P., Young, R.N., Zuercher, W.J., 2015. The promise and peril of chemical probes. Nat. Chem. Biol. 11, 536–541. http://dx.doi.org/10.1038/nchembio.1867.

Boilly, B., Boilly-Marer, Y., Bely, A.E., 2017. Regulation of dorso-ventral polarity by the nerve cord during annelid regeneration: a review of experimental evidence. Regeneration 4, 54–68. http://dx.doi.org/10.1002/reg2.78.

Boyle, M.J., Seaver, E.C., 2008. Developmental expression of *foxA* and *gata* genes during gut formation in the polychaete annelid, *Capitella* sp. I. Evol. Dev. 10, 89–105. http://dx.doi.org/10.1111/j.1525-142X.2007.00216.x.

Boyle, M.J., Yamaguchi, E., Seaver, E.C., 2014. Molecular conservation of metazoan gut formation: evidence from expression of endomesoderm genes in *Capitella teleta* (Annelida). Evodevo 5, 39. http://dx.doi.org/10.1186/2041-9139-5-39.

Brennan, J., Lu, C.C., Norris, D.P., Rodriguez, T.A., Beddington, R.S.P., Robertson, E.J., 2001. *Nodal* signalling in the epiblast patterns the early mouse embryo. Nature 411, 965–969. http://dx.doi.org/10.1038/35082103.

Chang, Y., Pai, C., Chen, Y., Ting, H., Martinez, P., Telford, M.J., Yu, J., Su, Y., 2016. Regulatory circuit rewiring and functional divergence of the duplicate *admp* genes in dorsoventral axial patterning. Dev. Biol. 410, 108–118. http://dx.doi.org/10.1016/j.ydbio.2015.12.015.

Clement, A.C., 1952. Experimental studies on germinal localization in *Ilyanassa*. I. The role of the polar lobe in determination of the cleavage pattern and its influence in later development. J. Exp. Zool. 121, 593–625. http://dx.doi.org/10.1002/jez.1401210310.

Clement, A.C., 1962. Development of *Ilyanassa* following removal of the D macromere at successive cleavage stages. J. Exp. Zool. 149, 193–215. http://dx.doi.org/10.1002/jez.1401490304.

Clement, A.C., 1976. Cell determination and organogenesis in molluscan development: a reappraisal based on deletion experiments in Ilyanassa. Am. Zool. 16, 447–453. http://dx.doi.org/10.1093/icb/16.3.447.

Corbet, M.B., Joyce, C., Sur, A., Renfro, A., Meyer, N.P., 2018. Function of BMP signaling in the annelid Capitella teleta and implication for nervous system evolution. Soc. Integr. Comp. Biol..

Damen, P., Dictus, W.J.A.G., 1996. Organiser role of the stem cell of the mesoderm in prototroch patterning in *Patella vulgata* (Mollusca, Gastropoda). Mech. Dev. 56, 41–60. http://dx.doi.org/10.1016/0925-4773(96)00510-2.

Dorresteijn, A.W.C., Wagemaker, H.A., Laat, S.W., Biggelaar, J.A.M., 1983. Dye-coupling between blastomeres in early embryos of *Patella vulgata* (mollusca, gastropoda): its relevance for cell determination. Wilhelm Roux's Arch. Dev. Biol. 192, 262–269. http://dx.doi.org/10.1007/BF00848658.

Dorresteijn, A.W.C., Bornewasser, H., Fischer, A., 1987. A correlative study of experimentally changed first cleavage and Janus development in the trunk of *Platynereis dumerilii* (Annelida, Polychaeta). Roux's Arch. Dev. Biol. 196, 51–58. http://dx.doi.org/10.1007/BF00376021.

Duboc, V., Röttinger, E., Besnardeau, L., Lepage, T., 2004. Nodal and BMP2/4 signaling organizes the oral-aboral axis of the sea urchin embryo. Dev. Cell 6, 397–410. http://dx.doi.org/10.1016/S1534-5807(04)00056-5.

Duboc, V., Röttinger, E., Lapraz, F., Besnardeau, L., Lepage, T., 2005. Left-right asymmetry in the sea urchin embryo is regulated by nodal signaling on the right side. Dev. Cell 9, 147–158. http://dx.doi.org/10.1016/j.devcel.2005.05.008.

Gaviño, M.A., Reddien, P.W., 2011. A Bmp/Admp regulatory circuit controls maintenance and regeneration of dorsal-ventral polarity in planarians. Curr. Biol. 21, 294–299. http://dx.doi.org/10.1016/j.cub.2011.01.017.

Gerhart, J., Danilchik, M., Doniach, T., Roberts, S., Rowning, B., Stewart, R., 1989. Cortical rotation of the Xenopus egg: consequences for the anteroposterior pattern of embryonic dorsal development. Development (107 Suppl), S37–S51.

Gerhart, J., Doniach, T., Stewart, R., 1991. Organizing the Xenopus Organizer. Plenum Press, New York.

Goldstein, B., Freeman, G., 1997. Axis specification in animal development. BioEssays 19, 105–116. http://dx.doi.org/10.1002/bies.950190205.

Grande, C., Patel, N.H., 2009. Nodal signalling is involved in left–right asymmetry in snails. Nature 457, 1007–1011. http://dx.doi.org/10.1038/nature07603.

Guerrier, P., van den Biggelaar, J.A.M., van Dongen, C.A.M., Verdonk, N.H., 1978. Significance of the polar lobe for the determination of dorsoventral polarity in *Dentalium vulgare* (da Costa). Dev. Biol. 63, 233–242. http://dx.doi.org/10.1016/0012-1606(78)90128-8.

Hao, J., Ho, J.N., Lewis, J.A., Karim, K.A., Daniels, R.N., Patrick, R., Hopkins, C.R., Lindsley, C.W., Hong, C.C., 2011. In vivo structure activity relationship study of dorsomorphin analogs identifies selective VEGF and BMP inhibitors. ACS Chem. Biol. 5, 245–253. http://dx.doi.org/10.1021/cb9002865.

Hejnol, A., 2010. A twist in time–the evolution of spiral cleavage in the light of animal phylogeny. Integr. Comp. Biol. 50, 695–706. http://dx.doi.org/10.1093/icb/icq103.

Henry, J.J., Martindale, M.Q., 1987. The organizing role of the D quadrant as revealed through the phenomenon of twinning in the polycheate *Cheatopterus variopedatus*. Roux's Arch. Dev. Biol. 196, 499–510. http://dx.doi.org/10.1007/BF00399874.

Henry, J.J., Perry, K.J., 2008. MAPK activation and the specification of the D quadrant in the gastropod mollusc, *Crepidula fornicata*. Dev. Biol. 313, 181–195. http://dx.doi.org/10.1016/j.ydbio.2007.10.019.

Henry, J.J., Klueg, K.M., Raff, R.A., 1992. Evolutionary dissociation between cleavage, cell lineage and embryonic axes in sea-urchin embryos. Development 114, 931–938.
Henry, J.Q., Perry, K.J., Martindale, M.Q., 2006. Cell specification and the role of the polar lobe in the gastropod mollusc *Crepidula fornicata*. Dev. Biol. 297, 295–307. http://dx.doi.org/10.1016/j.ydbio.2006.04.441.
Hopman, A.H.N., Ramaekers, F.C.S., Speel, E.J.M., 1998. Rapid synthesis of biotin-, digoxigenin-, trinitrophenyl-, and fluorochrome-labeled tyramides and their application for *in situ* hybridization using CARD amplification. J. Histochem. Cytochem. 46, 771–777. http://dx.doi.org/10.1177/002215549804600611.
Hover, L.D., Young, C.D., Bhola, N.E., Wilson, A.J., Khabele, D., Hong, C.C., Moses, H.L., Owens, P., 2015. Small molecule inhibitor of the bone morphogenetic protein pathway DMH1 reduces ovarian cancer cell growth. Cancer Lett. 368, 79–87. http://dx.doi.org/10.1016/j.canlet.2015.07.032.
Inman, G.J., Nicolás, F.J., Callahan, J.F., Harling, J.D., Gaster, L.M., Reith, A.D., Laping, N.J., Hill, C.S., 2002. SB-431542 is a potent and specific inhibitor of transforming growth factor-β superfamily type I activin receptor-like kinase (ALK) receptors ALK4, ALK5, and ALK7. Mol. Pharmacol. 62, 65–74.
Kenny, N.J., Namigai, E.K.O., Dearden, P.K., Hui, J.H.L., Grande, C., Shimeld, S.M., 2014. The Lophotrochozoan TGF-ß signalling cassette - diversification and conservation in a key signalling pathway. Int. J. Dev. Biol. 58, 533–549. http://dx.doi.org/10.1387/ijdb.140080nk.
Kimmel, C.B., Warga, R.M., Schilling, T.F., 1990. Origin and Organization of the Zebrafish Fate Map, vol. 594, pp. 581–594.
Koop, D., Richards, G.S., Wanninger, A., Gunter, H.M., Degnan, B.M., 2007. The role of MAPK signaling in patterning and establishing axial symmetry in the gastropod *Haliotis asinina*. Dev. Biol. 311, 200–212. http://dx.doi.org/10.1016/j.ydbio.2007.08.035.
Kraus, Y., Aman, A., Technau, U., Genikhovich, G., 2016. Pre-bilaterian origin of the blastoporal axial organizer. Nat. Commun. 7, 11694. http://dx.doi.org/10.1038/ncomms11694.
Kuo, D., Weisblat, D.A., 2011. A New Molecular Logic for BMP-Mediated Dorsoventral Patterning in the *Leech Helobdella*. Curr. Biol. 21, 1282–1288. http://dx.doi.org/10.1016/j.cub.2011.06.024.
de Laat, S.W., Tertoolen, L.G.J., Dorresteijn, A.W.C., van den Biggelaar, J.A.M., 1980. Intercellular communication patterns are involved in cell determination in early molluscan development. Nature 287, 546–548. http://dx.doi.org/10.1038/287546a0.
Lambert, J.D., Nagy, L.M., 2001. MAPK signaling by the D quadrant embryonic organizer of the mollusc *Ilyanassa obsoleta*. Development 128, 45–56.
Lambert, J.D., Nagy, L.M., 2003. The MAPK cascade in equally cleaving spiralian embryos. Dev. Biol. 263, 231–241. http://dx.doi.org/10.1016/j.ydbio.2003.07.006.
Lambert, J.D., Johnson, A.B., Hudson, C.N., Chan, A., 2016. Dpp/BMP2-4 mediates signaling from the D-quadrant organizer in a spiralian embryo. Curr. Biol. 26, 2003–2010. http://dx.doi.org/10.1016/j.cub.2016.05.059.
Lapraz, F., Haillot, E., Lepage, T., 2015. A deuterostome origin of the Spemann organiser suggested by Nodal and ADMPs functions in Echinoderms. Nat. Commun. 6, 8434. http://dx.doi.org/10.1038/ncomms9434.
Lartillot, N., Lespinet, O., Vervoort, M., Adoutte, A., 2002. Expression pattern of *Brachyury* in the mollusc *Patella vulgata* suggests a conserved role in the establishment of the AP axis in Bilateria. Development 129, 1411–1421.
Lee, S., Gilula, N.B., Warner, A.E., 1987. Gap junctional communication and compaction during preimplantation stages of mouse development. Cell 51, 851–860. http://dx.doi.org/10.1016/0092-8674(87)90108-5.
Lowe, C.J., Terasaki, M., Wu, M., Freeman, R.M., Runft, L., Kwan, K., Haigo, S., Aronowicz, J., Lander, E., Gruber, C., Smith, M., Kirschner, M., Gerhart, J., 2006. Dorsoventral patterning in hemichordates: insights into early chordate evolution. PLoS Biol. 4, 291. http://dx.doi.org/10.1371/journal.pbio.0040291.
Martindale, M.Q., 1986. The “organizing” role of the D quadrant in an equal-cleaving spiralian, *Lymnaea stagnalis* as studied by UV laser deletion of macromeres at intervals between third and fourth quartet formation. Int. J. Invertebr. Reprod. Dev. 9, 229–242. http://dx.doi.org/10.1080/01688170.1986.10510198.
Martín-Durán, J.M., Passamaneck, Y.J., Martindale, M.Q., Hejnol, A., 2016. The developmental basis for the recurrent evolution of deuterostomy and protostomy. Nat. Ecol. Evol. 1, 5. http://dx.doi.org/10.1038/s41559-016-0005.
Meyer, N.P., Seaver, E.C., 2009. Neurogenesis in an annelid: characterization of brain neural precursors in the polychaete *Capitella* sp. I.. Dev. Biol. 335, 237–252. http://dx.doi.org/10.1016/j.ydbio.2009.06.017.
Meyer, N.P., Seaver, E.C., 2010. Cell lineage and fate map of the primary somatoblast of the polychaete annelid Capitella teleta. Integr. Comp. Biol. 50, 756–767. http://dx.doi.org/10.1093/icb/icq120.
Meyer, N.P., Boyle, M.J., Martindale, M.Q., Seaver, E.C., 2010. A comprehensive fate map by intracellular injection of identified blastomeres in the marine polychaete *Capitella teleta*. Evodevo 1, 8. http://dx.doi.org/10.1186/2041-9139-1-8.
Molina, M.D., Neto, A., Maeso, I., Gómez-Skarmeta, J.L., Saló, E., Cebrià, F., 2011. Noggin and noggin-like genes control dorsoventral axis regeneration in planarians. Curr. Biol. 21, 300–305. http://dx.doi.org/10.1016/j.cub.2011.01.016.
Molina, M.D., de Crozé, N., Haillot, E., Lepage, T., 2013. Nodal: master and commander of the dorsal–ventral and left–right axes in the sea urchin embryo. Curr. Opin. Genet. Dev. 23, 445–453. http://dx.doi.org/10.1016/j.gde.2013.04.010.
Onai, T., Yu, J.-K., Blitz, I.L., Cho, K.W.Y., Holland, L.Z., 2010. Opposing Nodal/Vg1 and BMP signals mediate axial patterning in embryos of the basal chordate amphioxus. Dev. Biol. 344, 377–389. http://dx.doi.org/10.1016/j.ydbio.2010.05.016.
Pfeifer, K., Schaub, C., Domsch, K., Dorresteijn, A., Wolfstetter, G., 2014. Maternal inheritance of twist and analysis of MAPK activation in embryos of the polychaete annelid Platynereis dumerilii. PLoS One 9, e96702. http://dx.doi.org/10.1371/journal.pone.0096702.
Render, J., 1989. Development of *Ilyanassa obsoleta* embryos after equal distribution of polar lobe material at first cleavage. Dev. Biol. 132, 241–250. http://dx.doi.org/10.1016/0012-1606(89)90220-0.
Render, J.A., 1983. The second polar lobe of the *Sabellaria cementarium* embryo plays an inhibitory role in apical tuft formation. Wilhelm Roux's Arch. Dev. Biol. 192, 120–129. http://dx.doi.org/10.1007/BF00848680.
Rottinger, E., DuBuc, T.Q., Amiel, A.R., Martindale, M.Q., 2015. Nodal signaling is required for mesodermal and ventral but not for dorsal fates in the indirect developing hemichordate, *Ptychodera flava*. Biol. Open 4, 830–842. http://dx.doi.org/10.1242/bio.011809.
Schier, A.F., Shen, M.M., 2000. Nodal signalling in vertebrate development. Nature 403, 385–389. http://dx.doi.org/10.1038/35000126.
Schindelin, J., Arganda-Carreras, I., Frise, E., Kaynig, V., Longair, M., Pietzsch, T., Preibisch, S., Rueden, C., Saalfeld, S., Schmid, B., Tinevez, J.-Y., White, D.J., Hartenstein, V., Eliceiri, K., Tomancak, P., Cardona, A., 2012. Fiji: an open-source platform for biological-image analysis. Nat. Methods 9, 676–682. http://dx.doi.org/10.1038/nmeth.2019.
Seaver, E.C., Paulson, D.A., Irvine, S.Q., Martindale, M.Q., 2001. The spatial and temporal expression of Ch-en, the engrailed gene in the polychaete Chaetopterus, does not support a role in body axis segmentation. Dev. Biol. 236, 195–209. http://dx.doi.org/10.1006/dbio.2001.0309.
Seaver, E.C., Thamm, K., Hill, S.D., 2005. Growth patterns during segmentation in the two polychaete annelids, Capitella sp. I and Hydroides elegans: comparisons at distinct life history stages. Evol. Dev. 7, 312–326. http://dx.doi.org/10.1111/j.1525-142X.2005.05037.x.
Shen, M.M., 2007. Nodal signaling: developmental roles and regulation. Development 134, 1023–1034. http://dx.doi.org/10.1242/dev.000166.
Shih, J., Fraser, S.E., 1996. Characterizing the zebrafish organizer: microsurgical analysis at the early-shield stage. Development 122, 1313–1322.
Simakov, O., Marletaz, F., Cho, S.-J., Edsinger-Gonzales, E., Havlak, P., Hellsten, U., Kuo, D.-H., Larsson, T., Lv, J., Arendt, D., Savage, R., Osoegawa, K., de Jong, P., Grimwood, J., Chapman, J.A., Shapiro, H., Aerts, A., Otillar, R.P., Terry, A.Y., Boore, J.L., Grigoriev, I.V., Lindberg, D.R., Seaver, E.C., Weisblat, D.A., Putnam, N.H., Rokhsar, D.S., 2012. Insights into bilaterian evolution from three spiralian genomes. Nature 493, 526–531. http://dx.doi.org/10.1038/nature11696.
Spemann, H., Mangold, H., 1924. über induktion von embryonalanlagen durch implantation artfremder organisatoren. Arch. Mikrosk. Anat. Entwicklungsmech. 100, 599–638. http://dx.doi.org/10.1007/BF02108133.
Srivastava, M., Mazza-Curll, K.L., van Wolfswinkel, J.C., Reddien, P.W., 2014. Whole-body acoel regeneration is controlled by Wnt and Bmp-Admp signaling. Curr. Biol. 24, 1107–1113. http://dx.doi.org/10.1016/j.cub.2014.03.042.
Stewart, W.W., 1978. Functional connections between cells as revealed by dye-coupling with a highly fluorescent naphthalimide tracer. Cell 14, 741–759. http://dx.doi.org/10.1016/0092-8674(78)90256-8.
Tan, S., Huan, P., Liu, B., 2017. Expression patterns indicate that BMP2/4 and Chordin, not BMP5-8 and Gremlin, mediate dorsal–ventral patterning in the mollusk *Crassostrea gigas*. Dev. Genes Evol. 227, 75–84. http://dx.doi.org/10.1007/s00427-016-0570-3.
Vogt, J., Traynor, R., Sapkota, G.P., 2011. The specificities of small molecule inhibitors of the TGFß and BMP pathways. Cell Signal. 23, 1831–1842. http://dx.doi.org/10.1016/j.cellsig.2011.06.019.
Weiss, A., Attisano, L., 2013. The TGFbeta superfamily Ssignaling pathway. Wiley Interdiscip. Rev. Dev. Biol. 2, 47–63. http://dx.doi.org/10.1002/wdev.86.
Wu, M.Y., Hill, C.S., 2009. TGF-β superfamily signaling in embryonic development and homeostasis. Dev. Cell 16, 329–343. http://dx.doi.org/10.1016/j.devcel.2009.02.012.
Yamaguchi, E., Seaver, E.C., 2013. The importance of larval eyes in the polychaete *Capitella teleta*: effects of larval eye deletion on formation of the adult eye. Invertebr. Biol. 132, 352–367. http://dx.doi.org/10.1111/ivb.12034.
Yamaguchi, E., Dannenberg, L.C., Amiel, A.R., Seaver, E.C., 2016. Regulative capacity for eye formation by first quartet micromeres of the polychaete *Capitella teleta*. Dev. Biol. 410, 119–130. http://dx.doi.org/10.1016/j.ydbio.2015.12.009.
Yamaguchi, T.P., 2001. Heads or tails: Wnts and anterior–posterior patterning. Curr. Biol. 11, R713–R724. http://dx.doi.org/10.1016/S0960-9822(01)00417-1.